

# BARC

## NEWSLETTER

### IN THIS ISSUE

- Preparation, Characterization and Electrochemical Applications of Modified Electrodes
- Lattice Boltzmann Simulation to Study Reaction-Diffusion Processes in Geological Media
- Synthesis, characterization and photoluminescence spectroscopy of lanthanide ion doped oxide materials
- Design and Development of High Temperature  $^{10}\text{B}$  Coated Proportional Counters for PFBR
- Development of  $\text{Gd}_3\text{Ga}_3\text{Al}_2\text{O}_{12}:\text{Ce}$  Single Crystal Scintillator and USB Based Portable Gamma-ray Spectrometer



*Celebrating the spirit of Diamond Jubilee Year*

Department of Atomic Energy Tableau in the 66<sup>th</sup> Republic Day Parade 2015 at Rajpath, New Delhi



### *Atoms in the Service of the Nation*

Celebrating its diamond jubilee year, the Department of Atomic Energy (DAE) portrays in its tableau, its expertise in harnessing the tremendous potential of the atom for the benefit of the society. The tableau is led by a white dove atop an atomic orbital symbolizing the conviction of the nation in spreading the message 'Atoms for Peace'. It also pays homage to the visionary Dr. Homi Jehangir Bhabha, founding father of the Indian Nuclear Programme. The trailer portion of the tableau is conceptually divided into three parts depicting peace, progress and prosperity, vis-a-vis the service deliverables of the Department. The first part symbolizes progress in the field of medical technology depicting the indigenously developed 'Bhabhatron' machine, used in radiotherapy and delivering affordable health care. The colourful flora, following it, showcases prosperity in food and agriculture through mutation breeding technology to provide disease-resistant and high yielding seeds and food irradiation techniques that increase the shelf life of the produce. Lastly, standing tall, the indigenous Nuclear Reactor highlights the advantage of nuclear energy to provide an unlimited supply of clean and green energy for the sustained progress of the nation.

***Department of Atomic Energy***

## CONTENTS

<b>Editorial Note</b>	ii
<b>Research Articles</b>	
• Preparation, Characterization and Electrochemical Applications of Modified Electrodes Ruma Gupta and Suresh K. Aggarwal <i>Fuel Chemistry Division</i>	1
• Lattice Boltzmann Simulation to Study Reaction-Diffusion Processes in Geological Media T.K. Pal and R.S. Soni <i>Technology Development Division</i> and D. Datta <i>Health Physics Division</i>	6
• Synthesis, Characterization and Photoluminescence Spectroscopy of Lanthanide ion doped Oxide Materials Santosh K. Gupta and V. Natarajan <i>Radiochemistry Division</i>	14
<b>Technology Development Articles</b>	
• Design and Development of High Temperature $^{10}\text{B}$ Coated Proportional Counters for PFBR P.M. Dighe, D. Das, D.N. Prasad and L.P. Kamble <i>Electronics Division</i> and C.P. Nagaraj <i>Reactor Design Group, IGCAR, Kalpakkam</i> and R.K. Kaushik <i>Control Instrumentation Division</i> and S. Sarkar and S.S. Taliyan <i>Reactor Control Division</i> and P.P. Selvam, K. Binoy and N. Vijayan Varier <i>Technical Co-ordination &amp; Quality Control Division</i>	22
• Development of $\text{Gd}_3\text{Ga}_3\text{Al}_2\text{O}_{12}:\text{Ce}$ Single Crystal Scintillator and USB Based Portable Gamma-ray Spectrometer M. Tyagi, S.G. Singh, A.K. Singh, D.G. Desai, B. Tiwari, S. Sen, R. Datta, S.C. Gadkari and S.K. Gupta <i>Technical Physics Division</i>	33
<b>News &amp; Events</b>	
• Third National Symposium on Advances in Control and Instrumentation (SACI- 2014): a Report	39
• Theme Meeting on Application of Molecular Modeling in Separation Processes (AMMSP2015)	40
• Conference on Nanomaterials and Technologies (CNT-2014): a Report	41
• Report on DAE-BRNS 5 <sup>th</sup> Interdisciplinary Symposium on Materials Chemistry (ISMC – 2014)	42
• Report on Nineteenth National Symposium on Environment (NSE-19)	44
• Technology Transfer to Industries	46
• Report on 5 <sup>th</sup> Conference on Neutron Scattering (CNS2015)	49
• 59 <sup>th</sup> DAE Solid State Physics Symposium-2014	50
<b>BARC Scientists Honoured</b>	51

## Editorial Committee

### Chairman

Dr. S.M. Sharma,  
Associate Director, Physics Group

### Co-Chairman

Dr. G.K. Dey,  
Head, MSD

### Editor

Dr. G. Ravi Kumar  
Head, SIRD

### Associate Editors for this issue

Dr. A.K. Tyagi, Chemistry Divn.  
Dr. S. Kannan, FCD

### Members

Dr. G. Rami Reddy, RSD  
Dr. A.K. Tyagi, Chemistry Divn.  
Dr. S.M. Yusuf, SSPD  
Dr. S. Kannan, FCD  
Dr. C.P. Kaushik, WMD  
Dr. S. Mukhopadhyay, Seismology Divn.  
Dr. A.K. Bhattacharjee, RCnD  
Dr. B.K. Sapra, RP&AD  
Dr. J.B. Singh, MMD  
Dr. K.G. Bhushan, TPD  
Dr. S. Mukhopadhyay, ChED  
Dr. S.K. Sandur, RB&HSD  
Dr. Smt. S.C. Deokattey, SIRD

## From the Editor's Desk

On behalf of the new editorial committee headed by Dr. S. M. Sharma, I wish to welcome the readers to the 2015 edition of the BARC Newsletter. Some of the members of the new editorial committee, having been present in the previous committee, provide continuity. It is expected that the new members should be coming up with new ideas to the Newsletter. Cover page of this issue prominently features the DAE Tableau in this year's Republic Day parade in New Delhi, portraying the contributions of Department of Atomic Energy to the society.

This issue carries two technology development articles. One of the articles focuses on neutron detection using  $^{10}\text{B}$  coatings. In view of the prohibitive cost of  $^3\text{He}$  and its unavailability, it has become all the more important to pursue the  $^{10}\text{B}$  option for neutron detection. The other article discusses the development of a Photomultiplier Tube based on Cerium doped Gadolinium – Gallium Aluminate used in a portable Gamma - ray spectrometer powered by a laptop. In addition this issue carries three research articles. Further, we brought out brief reports on several conferences that were organized by BARC during the last few months.

Finally, I would like to welcome more contributions from the BARC scientists.

Dr. G. Ravi Kumar

On behalf of the Editorial Committee

# Preparation, Characterization and Electrochemical Applications of Modified Electrodes

Ruma Gupta and Suresh K. Aggarwal

Fuel Chemistry Division

## Abstract

Electrodes modified with metal nanoparticle, conducting polymer and carbon nanotubes were prepared and characterized. Diverse approaches were used for the modification of electrode surface, depositing metal nanoparticles and conducting polymer electrochemically studying their electrochemical behaviour in the absence and presence of analyte of interest. Modified working electrodes were much better in enhancing the reversibility and kinetics of the electrode processes compared to unmodified working electrode. These modified electrodes were applied for electrocatalytic reactions such as formic acid and methanol oxidation and also for studying the redox behavior of actinides. The intention of these studies was to utilize the modified electrodes for determination of actinides in the nuclear fuel samples and to mitigate the effect of CO poisoning in direct formic acid fuel cells (DFAFC) and direct methanol fuel cells (DMFC).

When considering an electrode designed for detection an analyte, one is interested in the following desired attributes: (i) surface development (ii) improved electrocatalysis and sensitivity (iii) freedom from surface fouling and (iv) exclusion of side reactions that might compete with the studied electrode process. All of above mentioned are difficult to achieve when only bare electrodes are taken into account. To overcome these limitations, researchers started to experiment with new, often complex materials and dedicated catalysts. Using them, they started to create so called modified electrodes. The branch of electrochemistry studying these newly developed electrodes has seen remarkable growth, and numerous important results have been achieved. Modified electrodes are designed and implemented in the field of electroanalytical detection to improve the sensitivity and selectivity of the system. In this respect, the electrode material is tailored specifically in such a way as to promote desired electrochemical reaction.

With the advent of nanotechnology, various new materials such as carbon-based nanomaterials, metals and metal oxide nanoparticles have emerged.

The uniqueness of nanomaterials when applied for electrode modification is based on their remarkable surface properties. Their surface to volume ratio increases with decrease in size. Such outcome leads to a well developed surface area and significant amelioration of sensitivity, electrical conductivity, and selectivity of the electrode modified with such materials. Also, there is a growing interest in the utilization of various kinds of conducting polymers to modify the physico-chemical properties of electrodes. Conducting electroactive polymers such as polyaniline, polypyrrole and polythiophene represent a new class of organic polymers that are capable of a range of interactions enabling them to interact with the species of interest.

Palladium nanoparticles modified electrode was prepared electrochemically in order to improve the performance of a Direct Formic Acid Fuel Cell (DFAFC) and Direct Methanol Fuel Cell (DMFC). Electroanalytical chemistry of uranium and plutonium in various supporting electrolytes (acidic, basic, and non-aqueous) at different electrodes (Hg, Pt, Ag, Au, graphite and glassy carbon) is well documented in literature. A limited number of publications

dealing with the applications of carbon nanotubes and conducting polymer modified electrodes for lanthanides and actinides electrochemistry are available. In the present work, we have investigated the electrochemistry of Pu(IV)/Pu(III) and U(VI)/U(IV) couples employing electrodes modified with SWCNTs and polyaniline. The study on electrochemical behaviour was then employed for simultaneous determination of U and Pu in Fast Breeder Test Reactor (FBTR) fuel samples by Voltammetry.

Neptunium (Np) is one of the actinides produced in nuclear reactors. It is located between U and Pu in the Periodic Table, suggesting that its chemical properties are qualitatively similar to those of U and Pu. Because of this chemical similarity as well as its considerable content in the spent nuclear fuels, the behavior of Np assumes importance in the fuel reprocessing process. Besides, the long half-life of  $^{237}\text{Np}$ ,  $2.14 \times 10^6$  years and high solubility of Np under environmentally relevant conditions makes it problematic on the long-term repository of radioactive wastes.

Synthesis of palladium nanoparticles on platinum electrode was carried out by employing a potentiostatic pulse method of electrodeposition [1]. The mechanism of electrocrystallization of PdNPs on Pt was investigated. Experimental results showed that Pd electrodeposition follows Volmer–Weber growth mechanism. The nucleation and growth phenomena in the initial stages of Pd deposition were investigated by potentiostatic transient measurements. Experimental current transients for 0.28V and 0.15V in a non-dimensional  $(i/i_{\text{max}})^2$  vs.  $t/t_{\text{max}}$  plot were compared with the theoretical curves. The transient at 0.15V fits relatively well with the theoretical curve for instantaneous nucleation. The electrodeposited PdNPs were characterized by X-ray photoelectron spectroscopy and Field emission scanning electron microscopy (FESEM). The results obtained suggested the presence of chemisorbed oxygen on the surface of PdNPs. The influence of

time of deposition on the size and monodispersity of the deposited PdNPs was investigated. The studies revealed that, the size of PdNPs increased with increase in the time of deposition. The effective catalytic surface area for the PdNPs/Pt was found to be  $0.197 \text{ cm}^2$ . The synthesized Pd nanoparticles modified Pt electrode displayed significantly different voltammetric behavior compared to bare Pt electrode and also showed high catalytic activity towards the electrooxidation of formic acid and methanol.

At polyaniline modified electrode, two systems were studied. Initially influence of ionic speciation on electrocatalytic performance of polyaniline

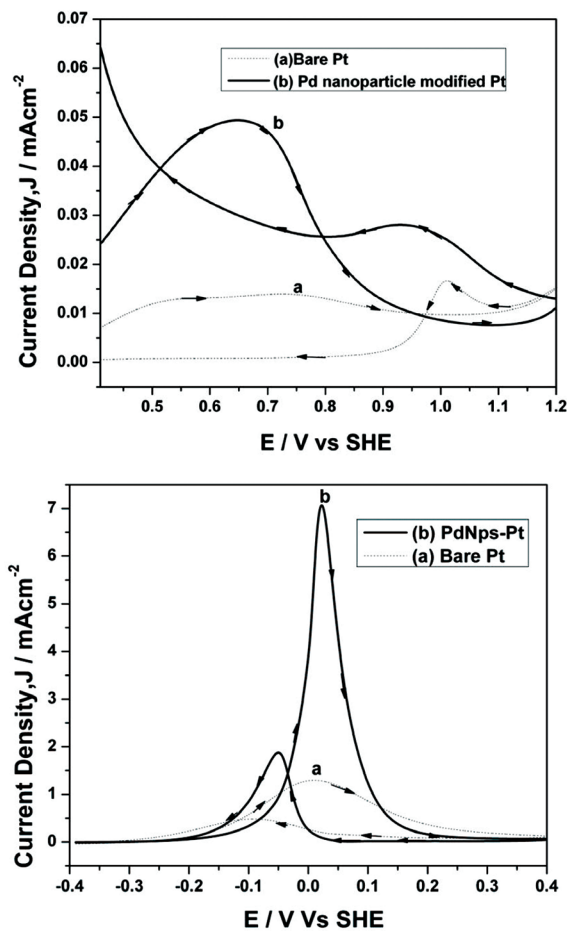
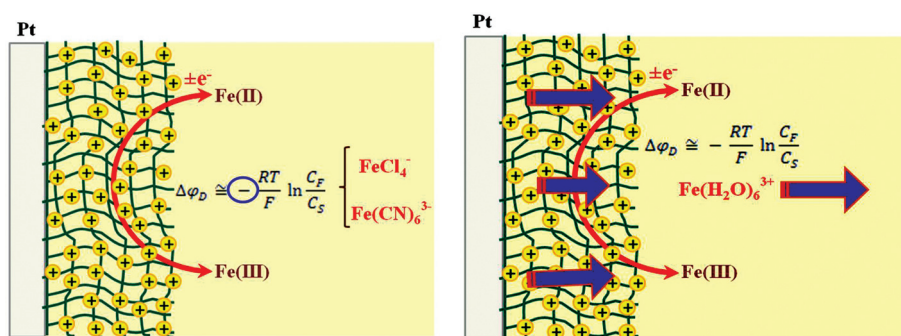


Fig. 1: Cyclic voltammograms (CVs) obtained at bare Pt electrode (curve a) and PdNPs modified Pt electrodes (curve b) (A) in 0.5 M  $\text{H}_2\text{SO}_4$  containing 0.5 M formic acid (B) in 0.5 M KOH containing 0.5 M methanol.



**Fig. 2: Schematics of the donnan interaction of different predominant species of different media with PANI matrix**

coated platinum electrode for Fe(III)/Fe(II) redox reaction was studied [2]. Porous-polyaniline coated Pt electrode (PANI/Pt) was electro-synthesized potentiodynamically. Nature of predominant Fe-species in HCl and H<sub>2</sub>SO<sub>4</sub> was checked by UV-vis spectrophotometry. Electrocatalysis of Fe(III)/Fe(II) reaction was studied by cyclic voltammetry (CV) and electrochemical impedance spectroscopy (EIS) for three different solution compositions viz. (i) FeCl<sub>3</sub>/FeCl<sub>2</sub> in 1M HCl, (ii) FeCl<sub>3</sub>/FeCl<sub>2</sub> in 0.5M H<sub>2</sub>SO<sub>4</sub> and (iii) Fe<sub>2</sub>(SO<sub>4</sub>)<sub>3</sub>/FeSO<sub>4</sub> in 0.5M H<sub>2</sub>SO<sub>4</sub>. The Donnan interaction of the polyaniline modified electrode for the three compositions was investigated with respect to [Fe(CN)<sub>6</sub>]<sup>3-</sup>/H<sub>2</sub>[Fe(CN)<sub>6</sub>]<sup>2-</sup> which are believed to be the predominant species present in K<sub>3</sub>[Fe(CN)<sub>6</sub>]/K<sub>4</sub>[Fe(CN)<sub>6</sub>] solution in 0.5M H<sub>2</sub>SO<sub>4</sub>. The electrocatalytic performance of PANI/Pt for Fe(III)/Fe(II) redox reaction was found to be superior in HCl compared to that in H<sub>2</sub>SO<sub>4</sub>.

The results indicate that ionic speciation of the diffusing redox species has a great influence on electrocatalytic behavior of polyaniline modified platinum electrode in mineral acid medium and the predominant redox ionic species existing in the solution is governed by the electrolytic composition. Based on the electrocatalytic behavior of PANI on Fe(III)/Fe(II) redox reaction and the effect of ionic speciation in the electrocatalysis mechanism, experiments were performed to study the electroanalytical performance of PANI for Pu(IV)/

Pu(III) couple [3]. There were two motivating aspects, firstly the redox potentials of Fe(III)/Fe(II) and Pu(IV)/Pu(III) couples are similar in 1 M H<sub>2</sub>SO<sub>4</sub> and secondly, the existence of Pu(IV) as an anionic complex in 1 M H<sub>2</sub>SO<sub>4</sub>. Detailed investigations were carried out to understand the

electrocatalytic mechanism of Pu(IV)/Pu(III) couple at the modified electrode. Further, a mechanistic study on the electrocatalysis of the Pu(IV)/Pu(III) redox reaction at a platinum electrode modified with polyaniline (PANI) was carried out. In this, electrochemistry of Pu(IV)/Pu(III) couple in 1 M H<sub>2</sub>SO<sub>4</sub> was studied on bare and modified platinum electrodes by cyclic voltammetry and electrochemical impedance spectroscopy. The platinum electrode was modified with polyaniline. The modified electrode was characterized by scanning electron microscopy and energy dispersive X-ray fluorescence. Electrocatalysis of Pu(IV)/Pu(III) redox reaction was observed on PANI-Pt. Pu(IV)/Pu(III) couple showed quasi-reversible electron transfer behavior on bare platinum electrode because of the PtO layer formation by Pu(IV) solution at the electrode-electrolyte interface. Electrocatalysis of Pu(IV)/Pu(III) couple on PANI-Pt was attributed to the cumulative effect of the Donnan interaction between PANI and Pu(IV) anionic complex, specific adsorption of Pu(IV) on the reactive centres, low charge transfer resistance across the electrode-electrolyte interface and a catalytic chemical reaction coupled with the electron transfer reaction.

Three redox couples were studied at SWCNT modified electrode. Firstly, mechanistic study on the electrocatalysis of Pu(IV)/Pu(III) redox reaction at platinum electrode modified with single-walled Carbon nanotubes (SWCNTs) was carried out [3].

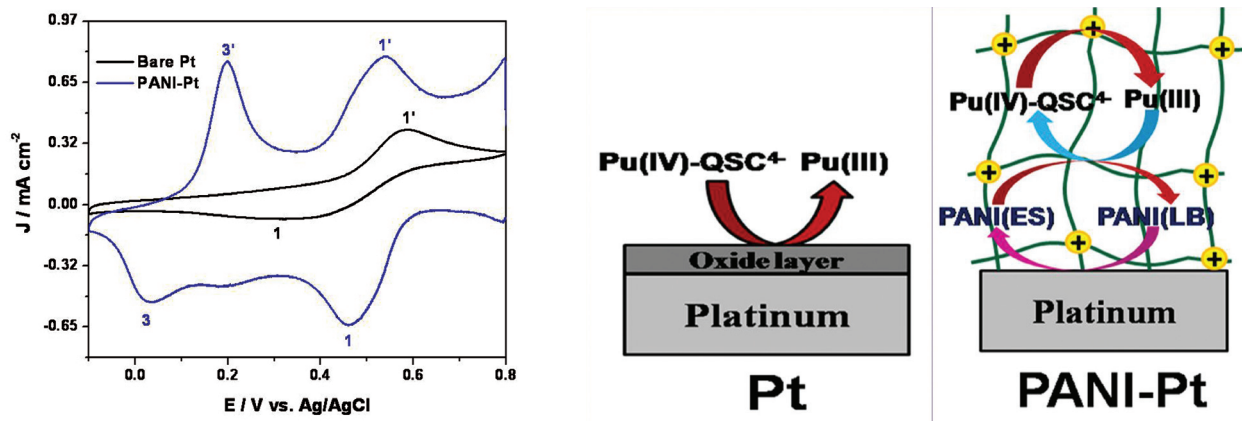


Fig. 3: (A) Cyclic voltammogram of 25 mM Pu(IV) in 1 M H<sub>2</sub>SO<sub>4</sub> solution on Pt and PANI-Pt electrodes at scan rate of 20 mV/s (B) Schematic of mechanism of the interaction of Pu with bare Pt and PANI/Pt

Electrocatalysis of Pu(IV)/Pu(III) redox reaction was observed on SWCNT-Pt. Pu(IV)/Pu(III) couple showed quasi-reversible electron transfer behavior on bare platinum electrode because of the PtO layer formation by Pu(IV) solution at the electrode-electrolyte interface. In SWCNT-Pt, the direct interaction between Pu(IV) and platinum was blocked by SWCNTs and it diminished the oxide layer formation at the interface. The lower charge transfer resistance at SWCNT-Pt also promoted the rate of electron transfer reaction of Pu(IV)/Pu(III) couple.

Electrochemical studies of U(VI)/U(IV) redox reaction in 1 M H<sub>2</sub>SO<sub>4</sub> at single-walled carbon nanotubes (SWCNTs) modified gold (Au) electrode was studied [4]. A detailed investigation was done to determine the kinetic parameters at the modified electrode. It was found that the electrocatalysis of U(VI)/U(IV) couple on SWCNT-Au is driven by an increase in the rate constant of the electron transfer reaction compared to that with the bare gold electrode. Electrochemical impedance spectroscopy data confirmed the electrocatalytic activity of SWCNT-Au electrode. After a detailed study on electrocatalytic mechanism of U(VI)/U(IV) couple and Pu(IV)/Pu(III) redox couple, studies were carried out to simultaneously determine Pu and U at SWCNT-Au electrode in the fuel samples

[5]. In the differential pulse voltammetry technique (DPV), both Pu and U gave sensitive reduction peaks at 564 mV and -128 mV, respectively, versus saturated Ag/AgCl electrode. Under the optimized experimental conditions, Pu and U gave linear responses over ranges of 10 to 100 μM (R<sup>2</sup> = 0.990) and 3 to 10 μM (R<sup>2</sup> = 0.987), respectively.

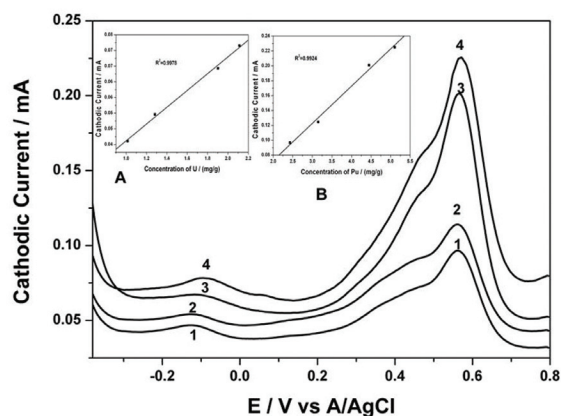


Fig. 4: DPV of various FBTR fuel samples containing different amount of Pu and U

The detection limits were found to be 8.2 μM for Pu and 2.4 μM for U.

The electrochemical investigations on Np(VI)/Np(V) redox couple using single walled carbon nanotube modified glassy carbon electrode (SWCNT-GC) were also carried out [6]. The peak-to-peak potential separation (ΔE<sub>p</sub>) was found to be 133 mV, which

is much smaller than the  $\Delta E_p$  value of 338 mV observed on bare glassy carbon electrode. It indicated that the Np(VI)/Np(V) couple still exhibits a quasi-reversible electron transfer behavior on SWCNT-GC. The increase of the redox peak current along with the significant enhancement in the electrochemical reversibility suggested the electrocatalytic action of SWCNT-GC for the Np(VI)/Np(V) redox reaction. The charge transfer coefficient ( $\alpha$ ) and the heterogeneous rate constant ( $k_s$ ) of Np(VI) reduction on SWCNT-GC in 1 M  $H_2SO_4$  were calculated as 0.83 and  $5.25 \times 10^{-1} \text{ cm s}^{-1}$ , respectively. This shows that the modification of glassy carbon surface with SWCNT catalyzed the Np(VI)/Np(V) redox reaction. Indeed, the SWCNT/GC electrode presents an interlinked highly mesoporous three-dimensional structure with a relatively higher electrochemically accessible surface area and easier charge transfer at the electrode/electrolyte interface. Therefore, the quasi-reversible redox reaction of Np(VI)/Np(V) couple on GC transformed to a more reversible redox reaction on SWCNT-GC. The impedance data on

charge transfer resistance ( $R_{ct}$ ) i.e.  $R_{ct}(\text{SWCNT-GC}) < R_{ct}(\text{GC})$  supported the trends of the heterogeneous rate constants calculated from the cyclic voltammetry experiments i.e.  $k_s(\text{SWCNT-GC}) > k_s(\text{GC})$ . This confirms the electrocatalytic behavior of SWCNT-GC for the Np(VI)/Np(V) redox reaction.

## References

1. Ruma Gupta, Saurav.K. Guin and Suresh K. Aggarwal, *Electrochimica Acta* 116 (2014) 314.
2. Saurav Guin, Ruma Chandra and S.K. Aggarwal, *Electrochimica Acta* 55 (2010) 8402.
3. Ruma Gupta, S.K Guin and S.K. Aggarwal, *RSC Advances* 2 (2012) 1810.
4. Ruma Gupta and S.K. Aggarwal, *Radiochimica Acta* 101 (2013) 399.
5. Ruma Gupta, Kavitha Jayachandran and S.K. Aggarwal, *RSC Advances* 3 (2013) 13491.
6. Ruma Gupta, J.V. Kamat and Suresh K. Aggarwal, *Radiochimica Acta* 102 (2014)1069.

# Lattice Boltzmann Simulation to Study Reaction-Diffusion Processes in Geological Media

T. K. Pal and R.S. Soni  
Technology Development Division  
*and*  
D. Datta  
Health Physics Division

## Abstract

A reaction-diffusion process of  $^{135}\text{Cs}$  diffusion through a sand column has been simulated using lattice Boltzmann simulation technique. Mathematical formulation of the reaction-diffusion process has been carried out where interaction of  $^{135}\text{Cs}$  with soil has been modeled as linear isotherm. The linear isotherm model converts reaction-diffusion problem to a diffusion problem with apparent diffusion coefficient instead of effective diffusion coefficient. Values of apparent diffusion coefficient for a particular Trombay soil has been taken from published literature data. A lattice Boltzmann diffusion model is used to simulate the process. Lattice Boltzmann solution is compared with analytical solution and a good agreement between the two is obtained. It has been shown that lattice Boltzmann simulation gives more accurate results as compared to finite difference method based solutions for the same time step value. Accuracy here is shown to be the closest to the analytical solution. Other superiorities of lattice Boltzmann method over convention numerical technique are highlighted with proper reasoning.

**Keywords:** Lattice Boltzmann, D1Q3, Diffusion-Reaction, Finite Difference Method

## Introduction

Disposal of vitrified high level radioactive waste canisters in a suitable geological formation is one of the most accepted technologies for management of high level radioactive waste. Worldwide different countries are working on different host rock formations, such as granite, basalt, clay stone etc. Though there is no operating deep geological repository for high level radioactive waste in any country, conceptual frame work of repository construction, operation and closure has been formulated [1]. A multi-barrier concept has been adopted for isolation of radionuclide from environment of human accessibility. It has been envisaged that after repository closure, groundwater may come in contact with waste canister and interact with it, which may lead to leaching of radionuclide from canister and subsequent migration through

groundwater. To suppress such processes, clay barriers are supposed to be put surrounding canisters. Clay being low permeable material will protect canisters from groundwater and its high sorption properties will be utilized for holding radionuclide in case of any accidental release of radionuclide from canisters. Clay barrier will also give mechanical stability against any disturbance due to earth quake. The host rock formation will function as a natural barrier for radionuclide migration. The safety assessment of nuclear waste disposal needs to predict the migration of radionuclide and chemical species through the multi-barriers system [2-3].

Migration of radionuclide through geological media is generally an effective process comprising of different individual processes such as, advection, diffusion, dispersion, bio-geochemical reactions,

decay of radionuclide etc. The effective process called reactive transport process [4] is not merely sum of individual processes rather it is the coupling of individual processes, for example long term geochemical interaction of groundwater with rock minerals may alter hydro-geological parameters (porosity, permeability etc.) of the host rock, which will alter ground water velocity and diffusivity. The variation in groundwater velocity and diffusivity will change contact time of radionuclide with host rock and therefore chemical process will also be altered [5-7]. Besides the challenges of addressing such diverse processes, there is an issue of scaling with geological porous material (host rock). Flow in such a media usually involves three scales: (a) the pore scale, (b) the representative elementary volume (REV) scale, and (c) the domain scale [8].

In clay rock, due to its low permeability reaction-diffusion process is the main controlling phenomenon that can lead to radionuclide to reach to environment of human accessibility [9]. Reaction-diffusion processes in geological porous media are basically pore scale phenomenon [10]. To address such process at pore scale, we need pore-scale models [4], which require detailed geometric information. The representative computational domain size for such model is limited to a relatively small scale and thus is not suitable for practical field applications. An alternative approach to overcome these limitations is to model the processes at Representative Elementary Volume (REV) scale, which is much larger than pore scale but much smaller than the field scale [11]. In fact REV works in the macroscopic domain. In view of this, we have taken volume averaged macroscopic equations which are governed by experimentally measurable parameters, such as porosity, permeability, dispersion coefficient etc. REV scale equations are numerically solved by traditional numerical techniques such as, Finite Difference Method (FDM), Finite Element method (FEM), Finite Volume Method (FVM) etc. Lattice Boltzmann method (LBM) is a newly developed

computational technique suitable for simulating fluid flow in complex geometries (porous material) [12-14]. LBM based reactive transport simulations, fluid flow coupled with chemical reaction in porous media are widely applied at pore scale [15-22], but considering the limitations of pore scale simulation as already explained, LBM has been used to simulate REV scale flow through porous media [23-28]. To apply LBM at REV scale, proper statistical modeling of the geometry is required to incorporate contribution of porous structure as a resistive field to the flow model [29].

In this study, geochemical interactions of solutes with rock materials are modeled as linear isotherms. Since simulation time is relatively small compared to geological time scale, time independent hydro-geological parameters are considered for the present study. It is also considered in this study that the rock mass is homogeneous (clay stone). All these assumptions convert reaction diffusion equation to a simple diffusion equation, and it is solved using standard lattice Boltzmann diffusion model. LBM has been chosen for solving the problem because of its simplicity and the inherent locality property. It has also been shown in this study that LBM based simulations yield more accurate results compared to FDM for the same time step value. The rest of the paper is organized in the following way: section 2 describes mathematics of the reaction-diffusion process. Section 3 gives general introduction to LBM and lattice Boltzmann (LB) model formulation for diffusion process. Results of computer simulations are given in section 4 and finally conclusion is discussed in section 5.

### Mathematical model

The geometry of model represents a column of porous rock material placed horizontally as shown in Fig 1. The process represents diffusion cell experiment to calculate diffusion coefficient of soil [30].

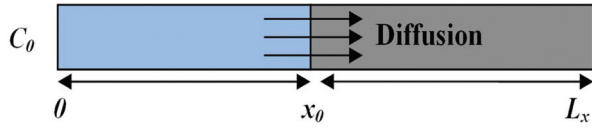


**Fig 1: Model geometry of the sand column**

<sup>135</sup>Cs was used to calculate the apparent diffusion coefficient of soil taken from different sites of Near Surface Disposal Facility (NSDF) in India for disposal of low and intermediate level radioactive waste [30]. <sup>135</sup>Cs being a very long lived radionuclide (half life  $2.3 \times 10^6$  yrs.) can be treated as non radioactive tracer for laboratory studies and calculated apparent diffusion coefficient can be used for short lived isotopes of cesium such as <sup>137</sup>Cs (half life 30.17 yrs.). Therefore, decay of radio nuclide has not been incorporated in this study. On the basis of Fick's law, single species diffusion equation at REV scale can be written as

$$\frac{\partial(\theta C(x,t))}{\partial t} = \frac{\partial}{\partial x} \left( \theta \cdot D_e \frac{\partial C(x,t)}{\partial x} \right) \quad (1)$$

where  $\theta$  is dimensionless porosity of the material,  $C$  is concentration of the species in the solution ( $ML^{-3}$ ),  $x$  is coordinate in  $x$  direction,  $D_e = D \cdot \varepsilon$  ( $L^2T^{-1}$ ) is effective diffusion coefficient, where  $D$  is diffusion coefficient of species in free water ( $L^2T^{-1}$ ) and  $\varepsilon$  is dimensionless tortuosity factor of the porous material. To incorporate reaction process in the diffusion model, one source/sink term is added to Eq. (1) as

$$\frac{\partial(\theta C(x,t))}{\partial t} = \frac{\partial}{\partial x} \left( \theta \cdot D_e \frac{\partial C(x,t)}{\partial x} \right) + S(x,t) \quad (2)$$

where  $S(x, t)$  is the space and time dependent source/sink term ( $ML^{-3}T^{-1}$ ) The form of  $S(x, t)$  depends on the reaction model considered for geo-chemical interaction. In this study, geochemical interactions are model as linear isotherms. Therefore, Eq. (2) takes the form as

$$\frac{\partial(\theta C(x,t))}{\partial t} = \frac{\partial}{\partial x} \left( \theta \cdot D_e \frac{\partial C(x,t)}{\partial x} \right) - \rho K_d \frac{\partial C(x,t)}{\partial t} \quad (3)$$

where  $\rho$  is bulk density of the soil ( $ML^{-3}$ ) and  $K_d$  is distribution coefficient of solute ( $L^3M^{-1}$ ), defined as the ration between mass of contaminant sorbed on unit mass of dry soil upon mass of contaminant in unit volume of solution at equilibrium stage. Due to homogeneity of the soil, we have uniform porosity and effective diffusivity; therefore,  $\theta$  and  $D_e$  are not space dependent parameter. Time dependency of hydro-geological parameters is not taken into consideration in this study; therefore,  $\theta$  and  $D_e$  are independent of time. With these assumptions, Eq. (3) can be simplified as

$$R_d \frac{\partial C(x,t)}{\partial t} = D_e \frac{\partial^2 C(x,t)}{\partial x^2} \quad (4)$$

where  $R_d$  is retardation factor of contaminant and can be defined as

$$R_d = \left( 1 + \rho \frac{K_d}{\theta} \right) \quad (5)$$

Simplified form of Eq. (4) can be written as

$$\frac{\partial C(x,t)}{\partial t} = D_x^* \frac{\partial^2 C(x,t)}{\partial x^2} \quad (6)$$

where  $D_x^* = D_e/R_d$  is known as apparent diffusion coefficient. Eq. (6) is a typical diffusion equation which can be solved numerically using LB diffusion model.

The initial and boundary conditions for the problem are

$$C(x,t) = 0 \text{ for } x_0 < x < L_x, t = 0 \quad (7)$$

$$= C_0 \text{ for } 0 < x < x_0, t = 0$$

$$\frac{\partial C(x,t)}{\partial x} = 0, \text{ at } x = 0 \text{ and } L_x \text{ for } t \geq 0 \quad (8)$$

where  $L_x$  is length of the soil column ( $L$ ),  $x_0$  is the offset distance (distance from extreme left to origin) ( $L$ ).  $C_0$  is initial concentration of <sup>135</sup>Cs ( $ML^{-3}$ ). Analytical solution

of Eq. (6) for the initial and boundary conditions (7) and (8) is given by Carslaw and Jaeger [31] as

$$\frac{c(x,t)}{c_0} = \frac{x_0}{L_x} + g(t) \cdot \cos\left(\frac{\pi mx}{L_x}\right) \sin\left(\frac{\pi mx_0}{L_x}\right)$$

where (9)

$$g(t) = \frac{2}{\pi} \sum_{m=1}^{\infty} \frac{\exp\left(-\frac{D_x^* m^2 \pi^2 t}{L_x^2}\right)}{m}$$

**Lattice Boltzmann Model**

LB approach is called particle-based or mesoscopic as it involves a finer description of physical quantities than the standard numerical techniques. The main idea behind the LBM is to treat fluid using statistical mechanics. In LB simulation, fictitious particles representing particle density distribution function are located at each lattice node of the domain. The dynamics of the particles follow Boltzmann transport equation. LB simulation is carried out by solving discrete lattice Boltzmann equation with Bhatnagar-Gross-Krook (BGK) [32] collision model. Based on the choice of lattice in LBM, different models are taken into considerations, e.g., for 1D, D1Q2, D1Q3 models, for 2D, D2Q4, D2Q5, D2Q9, and for 3D, D3Q15, D3Q19 etc. [14, 27]. Here for DnQm model n represent the dimension of the problem and m represent the number of discrete velocity vectors. Schematic of D1Q3 model is shown in Fig. (2).

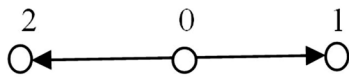


**Fig.2: D1Q3 model**

LB simulation of the problem is carried out using D1Q3 model, where 1 in D1 represent one dimensional problem and 3 in Q3 represent three discrete velocity components. The governing Lattice Boltzmann equation with BGK collision operator can be written as [32-33]

$$f_i(x + e_i \Delta t, t + \Delta t) = f_i(x, t) + \Omega_i^{BGK}(x, t) \tag{10}$$

$$\Omega_i^{BGK}(x, t) = \frac{\Delta t}{\tau} [f_i^{eq}(x, t) - f_i(x, t)] \tag{11}$$

where  $f_i(x, t)$  is density distribution function of the particle at point  $x$  at time  $t$  along  $i^{th}$  direction,  $f_i^{eq}(x, t)$  is equilibrium distribution function along  $i^{th}$  direction at  $x$  at  $t$ ,  $e_i$  is particle velocity along  $i^{th}$  direction,  $\Omega_i^{BGK}(x, t)$  is BGK collision operator in the  $i^{th}$  direction,  $\Delta t$  is discrete time step, and  $\tau$  is relaxation time. The velocity vector  $e_i$  for this model can be represented as

$$e_i = \begin{cases} 0, & i = 0 \\ (\cos(i - 1)\pi)e, & i = 1, 2 \end{cases} \tag{12}$$

where  $e = \Delta x / \Delta t$  ( $LT^{-1}$ ) and  $\Delta x$  is lattice size [ $L$ ]. Equilibrium distribution function,  $f_i^{eq}(x, t)$  of particles for advection-dispersion equation is given by [33]

$$f_i^{eq}(x, t) = w_i C(x, t) \left[ 1 + \frac{e_i \cdot u_x}{e_s^2} \right] \tag{13}$$

where  $u_x$  is macroscopic velocity along  $x$  direction ( $LT^{-1}$ ),  $w_i$  represents weight factor having values for a D1Q3 model as  $w_i = 4/6, 1/6,$  and  $1/6$  for  $i = 0, 1$  and  $2$  respectively. Speed of sound on lattice is  $e_s = e/\sqrt{3}$  [33]. For pure diffusion process,  $u_x = 0$  and therefore, equilibrium function takes the form

$$f_i^{eq}(x, t) = w_i C(x, t) \tag{14}$$

At this stage, we require to recover Eq. (6) from Eq. (10)-(11). Multi-scale Chapman-Enskog expansion technique can be utilized for this purpose. Using Chapman-Enskog expansion technique lattice diffusion coefficient can be recovered as [33]

$$D = e_s^2 \left( \tau - \frac{\Delta t}{2} \right) \tag{15}$$

Macroscopic particle density is calculated by summing over distribution functions as

$$C(x, t) = \sum_{i=0}^{i=2} f_i(x, t) \tag{16}$$

Eq. (10)-(11) can be solved numerically by LB algorithm which consists of following two processes [34].

**Streaming process**

In this process, particles move from one lattice point to nearest lattice point along the direction of the lattice velocity. Computationally this process is equivalent to swiping of computer memory. Algorithm of this process can be written as

$$f_i^*(x + e_i\Delta t, t + \Delta t) = f_i(x, t) \tag{17}$$

Here  $f_i^*(x + e_i\Delta t, t + \Delta t)$  represents nearest neighbor distribution function of  $f_i(x, t)$  along  $i$ th direction after the streaming process.

**Collision process**

In this process, particle distribution function relaxes towards local equilibrium distribution function. This process can be described by the following equations

$$f_i(x + e_i\Delta t, t + \Delta t) = f_i^*(x + e_i\Delta t, t + \Delta t) + \Omega_i^{BGK}(x + e_i\Delta t, t) \tag{18}$$

$$\Omega_i^{BGK}(x + e_i\Delta t, t) = \frac{\Delta t}{\tau} [f_i^{eq}(x + e_i\Delta t, t) - f_i^*(x + e_i\Delta t, t + \Delta t)] \tag{19}$$

Since particles reverse its direction after collision with obstacles or boundary walls, additional bounce-back boundary conditions [36] are imposed at obstacle sites and along boundary walls. Mathematically bounce-back algorithm can be written as

$$f_{i\pm 1}(x + e_i\Delta t, t + \Delta t) = f_i(x + e_i\Delta t, t + \Delta t) \text{ for } i = 1 \text{ and } 2 \text{ respectively} \tag{20}$$

Algorithm of LBM as written in Eq. (17)-(20) can easily be implemented in computer program [34]. It is worth to highlight here that computers perform arithmetic operations only in collision process

which is a localized operation. With a view to the computational framework of LBM it can be said that LB algorithm is suitable for parallel processing [36-39].

**Results and Discussions**

The simulation is performed in lattice units to maintain accuracy and stability of algorithm. In this simulation lattice spacing  $\Delta x$  is set to 1 in LB units and time step  $\Delta t$  is set to 1 time step in LB units. Accuracy of LB simulation depends on the value of  $\tau$  which can be in between 0.5 to 2 to obtain stable solution. Variation of output with  $\tau$  is shown in Fig. (3). It is observed that LB solution approaches to exact result when  $\tau$  approaches to 1. Therefore, in this simulation  $\tau$  is set to 1. Putting  $\tau = 1$  in Eq. (15), lattice diffusion coefficient  $D$  is estimated as  $1/6$ . Total lattice points  $N_x$  considered in the solution are taken as 100.

For mapping LB simulation to real world application, real world grid spacing is taken as  $dx = L/N_x = 10/100 = 0.1$  cm, where  $L = 10$  cm is the length of the diffusion cell. Corresponding time step for real world simulation can be estimated from following expression [40].

$$dt = \frac{dx^2}{6 D_x^*} \tag{21}$$

Numerical value of apparent diffusion coefficient is taken from literature [30]. Value for apparent diffusion coefficient for a particular Trombay soil is  $2.12 \times 10^{-11}$  m<sup>2</sup>/s. Time step value calculated from Eq. (20) is 7862 sec.

Computer programs for LBM algorithm, explicit FDM, and analytical solution are written in FORTRAN programming language. The simulations are run for time periods of 10, 30 and 60 days. Graphical representations of relative concentration profile of <sup>135</sup>Cs are shown in Fig. (4). Result shows that LB

solution is in good agreement with analytical solution, but explicit FDM solution differs slightly for the same time step size.

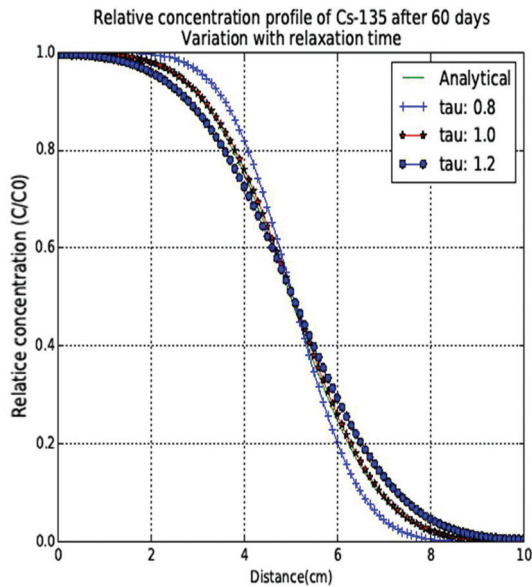


Fig.3: Variation of output with  $\tau$

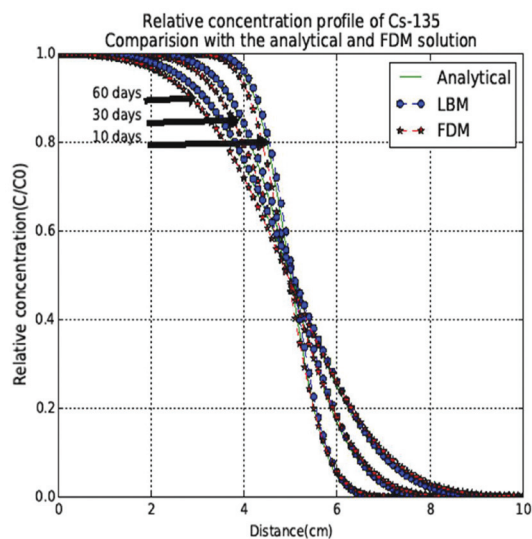


Fig. 4: Relative concentration of <sup>135</sup>Cs after 10, 30 and 60 days, comparisons with analytical and FDM solutions

**Conclusions**

The objective of this paper is to simulate macroscopic processes in geological media using LBM. We have simulated a simple process to test the suitability of

LBM. Our result shows that LB solution is closer to analytical solution compared to FDM result for same time step value. One can also change the lattice structure from D1Q3 to D1Q5 to improve the accuracy of the output, however computational load increases due to more degrees of freedom. Multi-component long term reactive transport simulations are versatile tool for assessment of long term durability of engineered barriers in deep geological repository. In this case, reaction part will be more complicated and simulation time should be of the order of 10<sup>4</sup> yrs. To address such processes external geochemical software such as, PHREEQC (commercial geochemical open-access software) is required to take care of reaction part of the simulation. Coupling between PHREEQC and LB diffusion model can be carried out using operator splitting approach generally used for multi-physics simulations. Considering the framework of LB algorithm, parallel programming techniques particularly domain decomposition method can be utilized to simulate computationally intensive problems.

**References**

1. W. R. Alexander, Linda McKinley, Deep Geological Disposal of Radioactive Waste. Amsterdam, the Netherlands: Elsevier (2007).
2. Hari S. Viswanathan, Bruce A. Robinson, Albert J. Valocchi, Ines R. Triay, A reactive transport model of neptunium migration from the potential repository at Yucca Mountain, *Journal of Hydrology.*, vol. 209(1-4), pp. 251-280 (1998).
3. Bernd Grambow, Sophie Bretesché, Geological disposal of nuclear waste: II. From laboratory data to the safety analysis – Addressing societal concerns, *Applied Geochemistry*, vol. 49, pp. 247-258 (2014).
4. Carl I. Steefel, Donald J. DePaolo, Peter C. Lichtner, Reactive transport modeling: An essential tool and a new research approach for the Earth

- sciences, *Earth and Planetary Science Letters*, vol. 240(3-4), pp. 539–558 (2005).
5. C.I. Steefel, A.C. Lasaga. A coupled model for transport of multiple chemical species and kinetic precipitation/dissolution reactions with application to reactive flow in single phase hydrothermal systems. *American Journal of Science*, vol. 294, pp. 529–592 (1994).
  6. Y. Le Gallo, O. Bildstein, E. Brosse, Coupled reaction-flow modeling of diagenetic changes in reservoir permeability, porosity and mineral compositions, *Journal of Hydrology*, vol. 209(1-4), pp. 366-388 (1998).
  7. Zysset, A., F. Stauffer, and T. Dracos, Modeling of chemically reactive groundwater transport, *Water Resour. Res.*, vol. 30(7), pp. 2217–2228 (1994).
  8. Neuman, S. P., Trends, prospects and challenges in quantifying flow and transport through fractured rocks, *Hydrogeol. J.*, vol. 13, pp. 124–147 (2005).
  9. Patriarche, D., E. Ledoux, J.-L. Michelot, R. Simon-Coinçon, and S. Savoye, Diffusion as the main process for mass transport in very low water content argillites: 2. Fluid flow and mass transport modeling, *Water Resour. Res.*, vol. 40, W01517 (2004).
  10. Li, L., C.I. Steefel, L. Yang, Scale dependence of mineral dissolution rates within single pores and fractures, *Geochimica Cosmochimica Acta*, vol. 72(2), pp. 360-377 (2008).
  11. Bear, J., *Dynamics of Fluids in Porous Media*, New York: Elsevier (1972).
  12. Succi, S., E. Foti, and F. Higuera, Three-dimensional flows in complex geometries with the lattice Boltzmann method, *Europhys. Lett.*, vol. 10(5), pp. 433-438 (1989).
  13. S. Chen and G. D. Doolen. Lattice Boltzmann method for fluid flows. *Annu. Rev Fluid Mech.*, vol. 30, pp. 329-364 (1998).
  14. Succi, S., *The Lattice Boltzmann Equation for Fluid Dynamics and Beyond*, Oxford, U. K.: Oxford Univ. Press (2001).
  15. Kang, Q., P. C. Lichtner, and D. Zhang, An improved lattice Boltzmann model for multicomponent reactive transport in porous media at the pore scale, *Water Resour. Res.*, vol. 43, W12S14 (2007).
  16. Kang, Q., P. Lichtner, H. Viswanathan, and A. Abdel-Fattah, Pore scale modeling of reactive transport involved in geologic CO<sub>2</sub> sequestration, *Transp. Porous Media*, vol. 82(1), pp. 197–213 (2010).
  17. A. Hiorth, E. Jettestuen, L.M. Cathles, M.V. Madland, Precipitation, dissolution, and ion exchange processes coupled with a lattice Boltzmann advection diffusion solver, *Geochim. Cosmochim. Acta*, vol. 104, pp. 99–110 (2013).
  18. C. Huber, B. Shafei, A. Parmigiani, A new pore-scale model for linear and non-linear heterogeneous dissolution, precipitation and sorption reactions, *Geochimica et Cosmochimica Acta*, vol. 124, pp. 109–130 (2013).
  19. L. Chen, Q. Kang, B.A. Robinson, Y.-L. He, W.-Q. Tao, Pore-scale modeling of multiphase reactive transport with phase transitions and dissolution-precipitation processes in closed systems, *Phys. Rev. E*, vol. 87(4), 043306 (2013).
  20. Chen, L., Q. Kang, B. Carey, and W.-Q. Tao, Pore-scale study of diffusion–reaction processes involving dissolution and precipitation using the lattice Boltzmann method, *Int. J. Heat Mass Transfer*, vol. 75, pp. 483–496 (2014a).
  21. Kang, Q., L. Chen, A. J. Valocchi, and H. S. Viswanathan, Pore-scale study of dissolution-induced changes in permeability and porosity of porous media, *J. Hydrol.*, vol. 517, pp. 1049–1055 (2014).
  22. L. Chen, Q. Kang, H.S. Viswanathan, W.-Q. Tao, Pore-scale study of dissolution induced changes

- in hydrologic properties of rocks with binary minerals, *Water Resour. Res.*, vol. 50, pp. 9343–9365 (2014).
23. D. M. Freed, Lattice-Boltzmann Method for Macroscopic Porous Media Modeling, *Int. J. Mod. Phys. C*, vol. 9, pp. 1491 – 1503 (1998).
  24. Z. Guo and T. S. Zhao, Lattice Boltzmann Model for Incompressible Flows through Porous Media, *Phys. Rev. E*, vol. 66, pp. 036304-1 – 036304-9 (2002).
  25. Q. Kang, D. Zhang, and S. Chen, Unified Lattice Boltzmann Method for Flow in Multi-scale Porous Media, *Phys. Rev. E*, vol. 66, pp. 056307-1 – 056307-11 (2002).
  26. S. Suga, Numerical schemes obtained from lattice Boltzmann equations for advection diffusion equations. *Int. J. Mod. Phys. C*, vol. 17, pp. 1563–1577, 2006.
  27. Sukop, M., and D. Thorne, Lattice Boltzmann Modeling: An Introduction for Geoscientists and Engineers, Heidelberg, Germany: Springer (2006).
  28. S. D. C. Walsh and M. O. Saar, Macroscale lattice-Boltzmann methods for low Peclet number solute and heat transport in heterogeneous porous media. *Water Resour. Res.*, vol. 46, pp. 1–15 (2010).
  29. Z. Guo, C. Zheng, B. Shi, Discrete lattice effects on the forcing term in the lattice Boltzmann method, *Phys. Rev. E*, vol. 65, pp. 046308-1-046308-6 (2002).
  30. Rakesh, R.R., Singh D.N., Nair R.N., A Methodology for simulating radionuclide diffusion in unsaturated soil, *Geotech. Geol. Eng.*, vol. 27, pp. 13-21 (2009).
  31. Carslaw, H.S., Jaeger, J.C., Conduction of heat in solids, 2nd Ed., Oxford: Oxford University Press (1959).
  32. E.G. Flekkøy, Lattice Bhatnagar–Gross–Krook models for miscible fluids, *Phys. Rev. E*, vol. 47, pp. 4247–4257 (1993).
  33. Wolf-Gladrow, D.A., Lattice-Gas Cellular Automata and Lattice Boltzmann Models: An Introduction. New York: Springer (2000).
  34. G. Wellein, T. Zeiser, G. Hager, S. Donath, On the single processor performance of simple lattice Boltzmann kernels. *Computers & Fluids*, vol. 35 (8-9), pp. 910-919 (2006).
  35. D. P. Zeigler, Boundary conditions for the lattice Boltzmann simulations, *J. Stat. Phys.*, vol. 71, pp. 1171-1177 (1993).
  36. Kandhai, D., A. Koponen, A. G. Hoekstra, M. Katajam, J. Timonen, and P. M. A. Slood, Lattice-Boltzmann hydrodynamics on parallel systems, *Comput. Phys. Commun.*, vol. 111, pp. 14–26 (1998).
  37. Wang, J., X. X. Zhang, A. G. Bengough, J. W. Crawford, Domain-decomposition method for parallel lattice Boltzmann simulation of incompressible flow in porous media, *Phys. Rev. E*, vol. 72(7), pp. 016706-1-016706-11 (2005).
  38. M. Wittmann, T. Zeiser, G. Hager, G. Wellein, Domain decomposition and locality optimization for large-scale lattice Boltzmann simulations, *Computer & Fluids*, vol. 80, pp. 283–289 (2013).
  39. M. Schulz, M. Krafczyk, J. Tölke, E. Rank. Parallelization strategies and efficiency of CFD computations in complex geometries using lattice Boltzmann methods on high-performance computers. High performance scientific and engineering computing, Berlin: Springer (2001), pp. 115–122.
  40. Ravi A. Patel, Janez Perko, Diederik Jacques, Geert De Schutter, Klaas Van Breugel, Guang Ye., A versatile pore-scale multi-component reactive transport approach based on lattice Boltzmann method: Application to portlandite dissolution, *Physics and Chemistry of the Earth, Parts A/B/C*; vol. 70–71, pp. 127–137 (2014).

# Synthesis, Characterization and Photoluminescence Spectroscopy of Lanthanide ion doped Oxide Materials

Santosh K. Gupta and V. Natarajan  
Radiochemistry Division

## Abstract

Main thrust of this work includes exploring lanthanide luminescence for structural probe, synthesizing white light emitting materials and understanding defect induced emission in nanomaterials. Refractory materials like zirconia and thoria doped with  $\text{Eu}^{3+}$  have been synthesized at a low temperature using reverse micellar route and investigated the photoluminescence properties of Eu doped  $\text{ThO}_2$  and  $\text{ZrO}_2$ . Luminescence properties of Eu, Dy and Sm in strontium silicate and their local site occupancy have been described. EXAFS measurements and theoretical calculations have been carried out to justify the experimental results. In  $\text{SrZrO}_3$ , PL findings show that  $\text{Eu}^{3+}$  ions occupy both  $\text{Sr}^{2+}$  and  $\text{Zr}^{4+}$  sites and their spectral characteristics are entirely different. Optical properties of Sm, Gd and Dy doped  $\text{SrZrO}_3$  have also been discussed. Rare earth free blue emitting  $\text{Sr}_2\text{CeO}_4$  has also been synthesized. An entirely new phosphate based phosphor; zinc pyrophosphate has been explored. The effect of zinc coordination on the photophysical properties of lanthanide and transition metal ion was also studied.

Optical materials doped with rare earth elements are of great relevance in science and technology. Modern solid state optical technology is mainly based on lanthanide doped materials, with applications ranging from solid state lighting, field emission diodes, in-vivo fluorescence imaging, white-light-emitting phosphor for UV-LEDs, finger print detection, proton detector, lasers, dosimetry, drug delivery and optical & MRI imaging. From the scientific point of view, lanthanide doped materials attract increasing attention due to their particular physical properties. In the context of global energy shortage, energy-saving is an important issue. In the field of lighting, white light emitting diode (WLED), a new generation solid source has been highlighted due to its high luminous efficiency, low energy consumption and great potential in environmental protection. Thereafter there is a present trend to replace the traditional incandescent and fluorescent lamps. There is a tremendous growth in the development of WLED worldwide due to its various applications viz. lighting, motor vehicle and backlight for mobile panel and liquid crystal displays.

Luminescent dopants are also extensively used as local probes for identifying local structures in crystalline material, understanding the effect of chemical and thermal treatment on catalysts and probing the structure of biological molecules. In view of its non-degenerate emissive state,  $^5\text{D}_0$ , Eu (III) ion is most appropriate as a luminescent structural probe for the determination of the number of metal ion sites in a compound, their symmetry, and their respective population. Other lanthanide ions have transitions that are usually the mixtures of electric dipole transition (EDT) and magnetic dipole transition (MDT) and the effects of symmetry are less pronounced.

Because of unique spectroscopic properties and luminescent dynamics of f-electron states, doping luminescent rare earth ions into nano-hosts has been demonstrated as an optimistic approach to develop highly efficient and stable nanophosphors for various applications. Compared to bulk materials, nanoparticles exhibit greater electron-hole overlap, thereby yielding greater oscillator strength and

enhanced luminescence quantum efficiency. Improved oscillator strength is important because a phosphor's emission decay lifetime is inversely proportional to its oscillator strength and typically shortens as particle size decreases. Similarly, by overcoming the inherent loss of luminescence efficiency normally associated with smaller size materials, luminescence nanoparticles hold the promise of practical phosphors that are considerably smaller than what can be achieved currently. Among the materials evaluated as hosts for lanthanide ions in this work, our attention was mostly focused on alkaline earth silicate, zirconate and cerate. These materials are characterized by good transmission properties in the visible part of the electromagnetic spectrum and relatively low phonon energies. They can be efficiently doped with lanthanide ions, due the similarity between the ionic radius of the alkaline earth and the lanthanide ions. Therefore these materials are prospective high efficiency luminophors and are attracting increasing interest for photonics and optoelectronics applications. Indeed alkaline earth silicate, zirconate and cerate are resistant to many chemicals and air exposure. They can also be grown with low-cost techniques. They are also thermally, chemically and mechanically stable. Few new oxide hosts were also tried to venture into novel lanthanide doped luminescent materials viz.  $Zn_2P_2O_7$ ,  $ThO_2$  and  $ZrO_2$ .

We have also synthesized some novel white light emitting materials with high CRI index and efficiency. The idea is to synthesize low phonon-energy luminescent materials (micro and nano regime) to minimize non-radiative losses.

Various synthesis techniques were explored to synthesize the nanoparticles viz. Sol-gel, combustion, polymeric precursor, reverse micellar etc. Characterization of the materials is done by various physical and chemical methods. For structure, phase purity and crystallite size, X-Ray

Diffraction has been used. For morphology and average particle size electron microscopy has been used. Dynamic light scattering (DLS) has been used for calculating particle size distribution and hydrodynamic radii. Extended X-ray absorption fine structure (EXAFS) is used to understand the local environment around  $Ln^{3+}$  ion in various inorganic hosts. Positron annihilation spectroscopy (PAS) is used to understand the nature of defects which arises due to aliovalent substitution. TRES has been extensively used in this work for recording such as emission and excitation spectra and luminescence lifetimes.

Synthesizing nanoparticles of refractory oxides like  $ThO_2$  and  $ZrO_2$  at lower synthesis temperature is a challenge [1-4]. Through the present work, we have tried to investigate the emission, excitation and lifetime studies of the samarium/europium ion in thoria matrix. The sites occupied by  $Sm^{3+}$  ions and effect of site symmetry were studied using time resolved emission spectrometry. PL spectra of  $Eu^{3+}$ :  $ThO_2$  nanocrystals were studied after annealing at higher temperatures in the range 500-900°C.  $Eu^{3+}$  ion occupied two different sites in the host and relaxes at different time intervals [1]. Nanorods of thoria emit in blue region [2] whereas warm white light emission in  $ThO_2:Sm^{3+}$  and intense red emission in case of  $ThO_2:Eu^{3+}$  [3] is observed. Biexponential decay is observed for  $Sm^{3+}$  as well as for  $Eu^{3+}$  in  $ThO_2$ . Longer lived species are due to the presence of  $Sm^{3+}/Eu^{3+}$  ion in cubic (Oh) site with inversion symmetry. Shorter species are due to their presence on the surface of nanocrystals in case of  $ThO_2:Sm^{3+}$  and in non-cubic ( $C_2$ ) site in case of  $ThO_2:Eu^{3+}$ . In case of  $ThO_2:Eu^{3+}$ ; extent of asymmetry around  $Eu^{3+}$  at 700/900°C is very high as compared to as prepared or 500°C annealed sample and also this gets reflected in percentage of long lived species. Pictorial representation of site symmetry around europium in nano and bulk thoria is shown in Fig. 1.

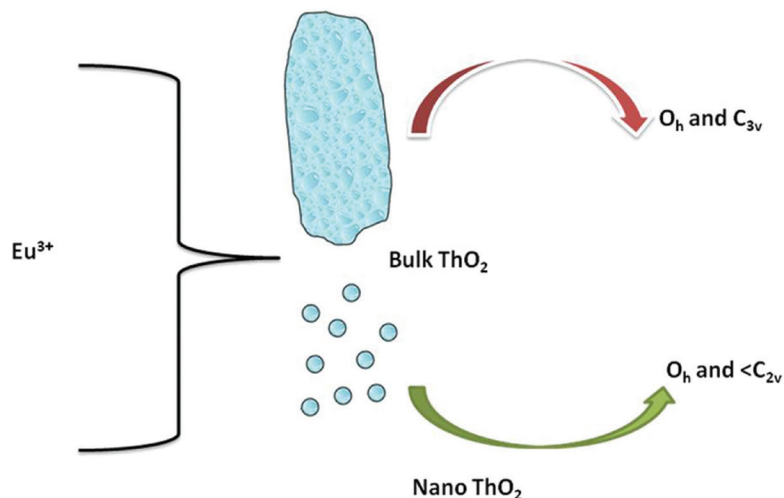


**Fig. 1: Schematics of site symmetry around europium ions in nano and bulk thoria**

As far as  $ZrO_2:Eu^{3+}$  is concerned; this is the first report on synthesis of zirconia using non-ionic surfactant in reverse micelle. Through this route, we could stabilize metastable tetragonal phase at 500°C through the addition of 1 mol %  $Eu^{3+}$ , which is technologically more important [4] shown in Fig. 2. Hosts like  $ThO_2$ ,  $Zn_2P_2O_7$  and  $Sr_2CeO_4$  having very low phonon energy and in turn are good candidates

as luminescent materials; but they are relatively unexplored. Another novel approach is to use lanthanide ion as a structural probe (structure- properties correlation). Further understanding why different lanthanides (Sm, Eu and Dy) behave differently in same host is an interesting problem. This can be solved by theoretical validation of experimental results.

Although reports exist on luminescence properties of lanthanide ion in  $Sr_2SiO_4$  and  $SrZrO_3$  (SZ), none of them explain the site occupancy of  $Ln^{3+}$  and its related effect on luminescence properties in these matrices. When an active dopant is introduced into host with multiple sites, the optical and magnetic properties are dramatically changed depending on the distribution of the dopant in the perovskite ceramic. Studies of dopant ion distribution in such materials have attracted much attention, because they may lead to better understanding of the correlations between

structure and properties such as color, magnetic behavior, catalytic activity, and optical properties, etc., which are strongly dependent on the occupation of these two sites by metal ions. Time resolved emission spectroscopy (TRES) is extensively used as a tool to understand such phenomena. In this context  $Sr_2SiO_4$  has attracted current interest due to its special structural features and potential application in developing white light-emitting-diodes (LEDs), because GaN (400 nm chip) coated with  $Sr_2SiO_4 : Eu^{2+}$  exhibits better luminous efficiency than that of industrially available products such as InGaN (460 nm chip) coated

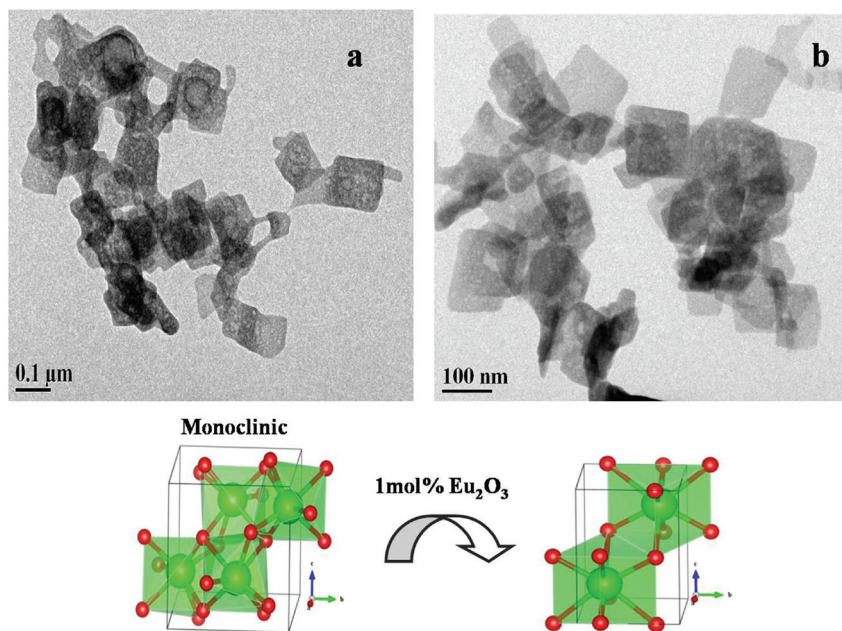


**Fig. 2: TEM micrographs of zirconian nanocubes and monoclinic to tetragonal phase transition in  $ZrO_2$**

with YAG : Ce . In the structure of  $Sr_2SiO_4$ , there are two different Sr sites: one having coordination number 9 and the other with coordination number 10. The ten coordinated Sr(1) sites form linear three-membered rows of (Si–O–Sr(1)–O–Sr(2)), whereas the nine coordinated Sr(2) sites form zig-zag chains of (Sr(1)–O–Sr(2)–O–Sr(1)) along the b-axis . Sr (1) polyhedron has more symmetric environment with hexagonal pseudo-symmetry along the y-axis. It shares the face and the vertex with the two  $SiO_4$  tetrahedra, which are vertically above and below it and the three edges with three  $SiO_4$  tetrahedra. We have doped 0.5 mol % Eu, Dy and Sm in  $Sr_2SiO_4$  [5-8]. TRFS studies showed that that Eu(III)/Eu(II) occupy both Sr(1) and Sr(2) sites, whereas Dy and Sm occupy only Sr(2). Theoretical calculations were done to validate the experimental results. Theoretical calculation showed that energetically substitution of  $Sr^{2+}$  by Eu in  $Sr_2SiO_4$  at 9-coordinated site is more favorable than at 10-coordinated site. Due to relatively higher bond strength of Dy-O and Sm-O bonds, the inclusion of these at 10-coordinated site results in shortening of few M-O bonds, which leads

to distortion in MO10 polyhedra. Such a distortion leads to destabilization of the conformer having Dy/Sm ion at 10-coordinated sites.

As far as  $SrZrO_3$  (SZO) perovskite is concerned; none of the available literature explained the site symmetry of  $Ln^{3+}$  in  $SrZrO_3$  nanocrystals. Considering the relatively wide band gap, high refractive index and lower phonon energy, SZO is a good candidate to be used as the host material in order to excite RE ions efficiently and to yield intense luminescence. Metal ions could be conveniently substituted into the SZO lattice, if their ionic radii are comparable to that of the  $Sr^{2+}/Zr^{4+}$  cations. It is thought that these “magic” dopants can choose their site occupancy as a result of the local Sr/Zr ratio and oxygen partial pressure during firing. Such dopants are also termed “amphoteric”, because the site change of a dopant with well defined valence causes a change of the relative charge. The  $ABO_3$  type perovskites having various crystalline structures show interesting physiochemical properties and is a potential host for the chemical substitution. Substitution at both A and B sites can

lead to change in symmetry and composition and thus create various defects viz. cation or oxygen vacancies, which can drastically influence the band structures and this is the main factor in determining the electronic structures. In particular, these materials can accommodate lanthanide ions at the A-site or B-site, and these doped oxides are not only used as probes to investigate local centers and energy, but also to provoke changes in their optical behavior. Moreover, doping foreign elements into a semiconductor with a wide

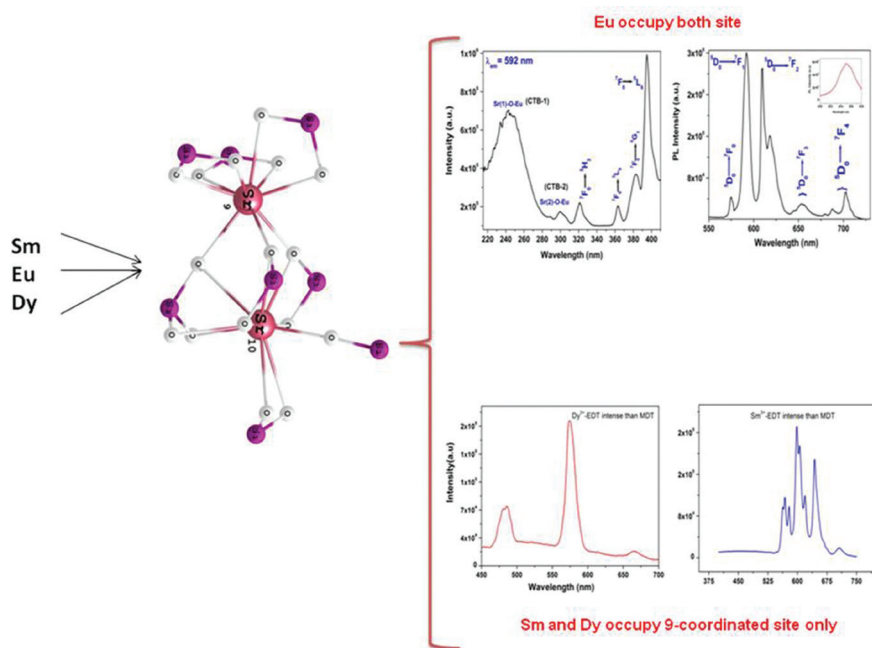


Fig. 3: Site occupancy of Sm, Eu and Dy in  $Sr_2SiO_4$

band gap to create a new optical absorption edge is known to be one of the primary strategies for developing materials with optical-driven properties.

Nanocrystalline SZO sample showed defect induced intense violet blue and weak orange red emissions. Based on EPR and theoretical studies, these defects were attributed to the presence of shallow and deep defects respectively. Their corresponding lifetimes were calculated using PL decay measurements.

However, the role of the rare earth (RE) in the perovskite structure is not very clear and is still being discussed. We have doped 0.5 mol % of Eu, Sm Gd and Dy in SZO and exploited time resolved photoluminescence to understand their local site in the same [9-12]. On doping  $\text{Sm}^{3+}$  in SZO, an efficient energy transfer takes

place and  $\text{Sm}^{3+}$  ions are localized both at Sr and Zr positions of SZO and is shown pictorially in Fig. 4. Theoretical calculation has shown that incorporating Sm at individual site does not change the band gap at all; but incorporating Sm simultaneously at Sr and Zr site decreases the band gap by 0.7 eV. PL decay time showed the presence of two life times in case of nanocrystalline  $\text{SrZrO}_3:\text{Sm}^{3+}$ : (i)  $\text{Sm}^{3+}$  at  $\text{Zr}^{4+}$  site ( $\tau=500 \mu\text{s}$ ) and (ii)  $\text{Sm}^{3+}$  at  $\text{Sr}^{2+}$  site ( $\tau=1.2 \text{ ms}$ ) in the ratio of 3:1. In europium doped SZO sample also, europium is distributed between two sites, Sr and Zr; HAB (host absorption band) excites mostly Eu ion at Sr site, CTB (charge transfer band) excites mostly Eu ion at Zr site, whereas f-f band excites both Eu ions at Sr and Zr sites equally. However Gd ion prefers  $\text{Sr}^{2+}$  sites and Dy ion prefers  $\text{Zr}^{4+}$  site only in SZO.

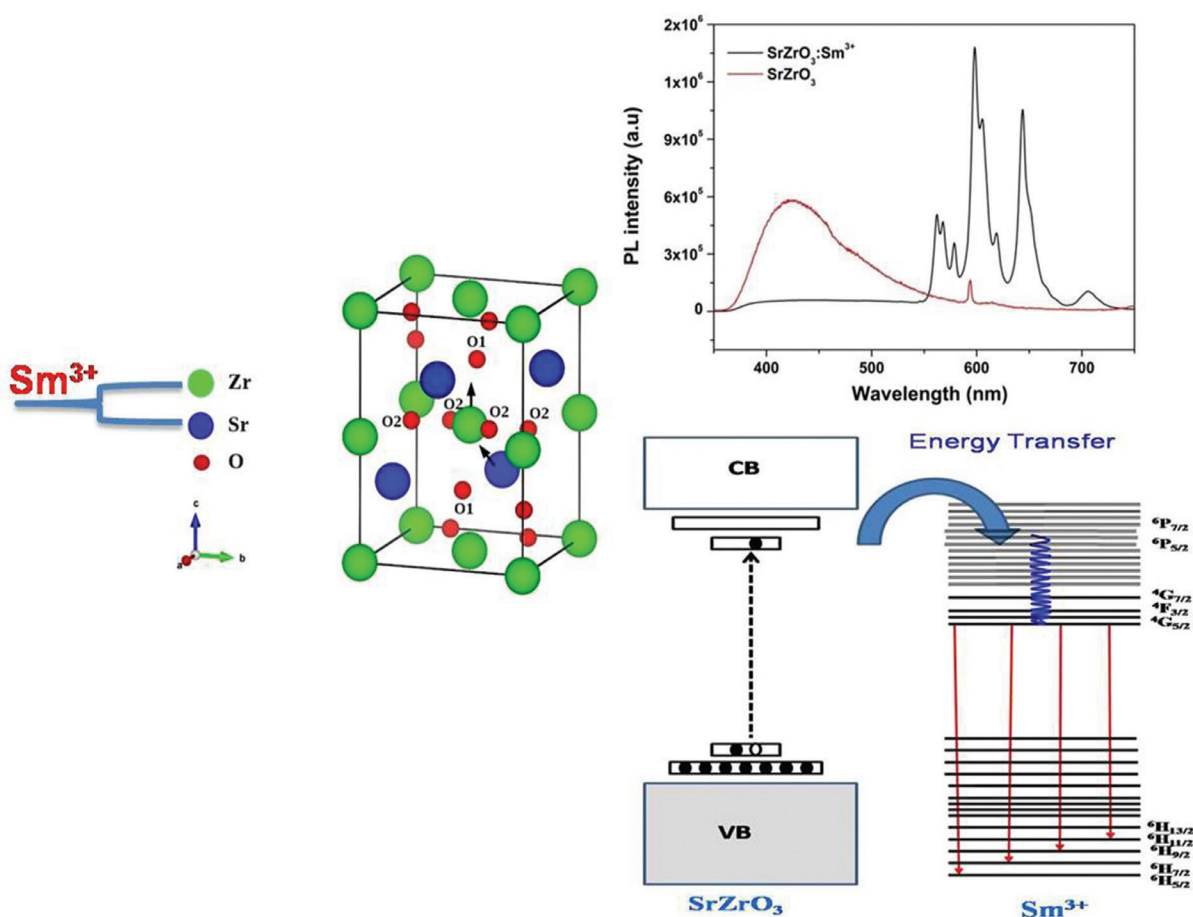


Fig. 4: Localization of  $\text{Sm}^{3+}$  ion and energy transfer from host to  $\text{Sm}^{3+}$  ions in  $\text{SrZrO}_3$  nanocrystal

Different lanthanide ions viz. Eu, Sm and Dy ions have been used as structural probes to understand their site occupancy in  $\text{Sr}_2\text{SiO}_4$  and  $\text{SrZrO}_3$ . These ions were found to behave differently in terms of their local site occupancy in these matrices. This aspect has been investigated in detail in the present work. Theoretical modeling and EXAFS studies were carried out to explain such anomaly. Effect of replacing Si (IV) by Ce (IV) in  $\text{Sr}_2\text{SiO}_4$  is investigated in  $\text{Sr}_2\text{CeO}_4$  system. Ionic size of silicon 0.40 Å; not ideal for  $\text{Eu}^{3+}$  substitution- entire Eu occupy  $\text{Sr}^{2+}$  site. Si (IV) is replaced by Ce (IV) whose ionic radius is very close to Eu (III). Also synthesizing  $\text{Sr}_2\text{CeO}_4$  is difficult, because it decomposes peritectically to SrO and  $\text{SrCeO}_3$  at higher temperatures. The concentration of the dopant ion optimized for maximum PL intensity. Effect of concentration on excitation, emission and lifetime spectroscopy was investigated in details. The critical energy-transfer distance for the  $\text{Eu}^{3+}$  ions was evaluated based on which, the quenching mechanism was verified to be a multipole–multipole interaction [13]. Emission spectrum at each concentration and energy transfer mechanism is shown in Fig. 5.

Luminescence properties of hosts like  $\text{Zn}_2\text{P}_2\text{O}_7$  (both undoped and doped) with lanthanide ions have been investigated for the first time with a view to develop new and robust phosphor materials

having multifunctional applications. Novel  $\text{Sm}^{3+}$  doped  $\text{Zn}_2\text{P}_2\text{O}_7$  white emitting material has been synthesized [14]. Zinc pyrophosphate is known to undergo structural phase transition at 132°C. We have doped 2.0 mol %  $\text{Mn}^{2+}$  in zinc pyrophosphate and used electron paramagnetic resonance (EPR) as a probe to understand the mechanism for phase transition [15, 16]. This aspect was also supported by high temperature x-ray diffraction (HTXRD) and differential scanning calorimetry (DSC). Photophysical properties of europium doped zinc pyrophosphate were studied in detail.

PL Emission and decay time data of the sample suggested the stabilization of the  $\text{Eu}^{3+}$  ion at two different sites. The first type was a long lived species ( $\sim t = 1.77$  ms) present at asymmetric ‘5-coordinated Zn (S1)’ sites and the second was a short lived component ( $t = 620$  ms) present at relatively symmetric ‘6-coordinated Zn (S2) sites [17]. Emission pertaining two sites is shown in Fig. 6.

A low temperature experiment does not give any light on this except the enhancement in emission intensity and decay time. This unusual phenomenon is explained by-calculating theoretical value of radiative lifetime-Judd-Ofelt (J-O) calculations. Radiative life time of the  $\text{Eu}^{3+}$  species present in symmetric environment was

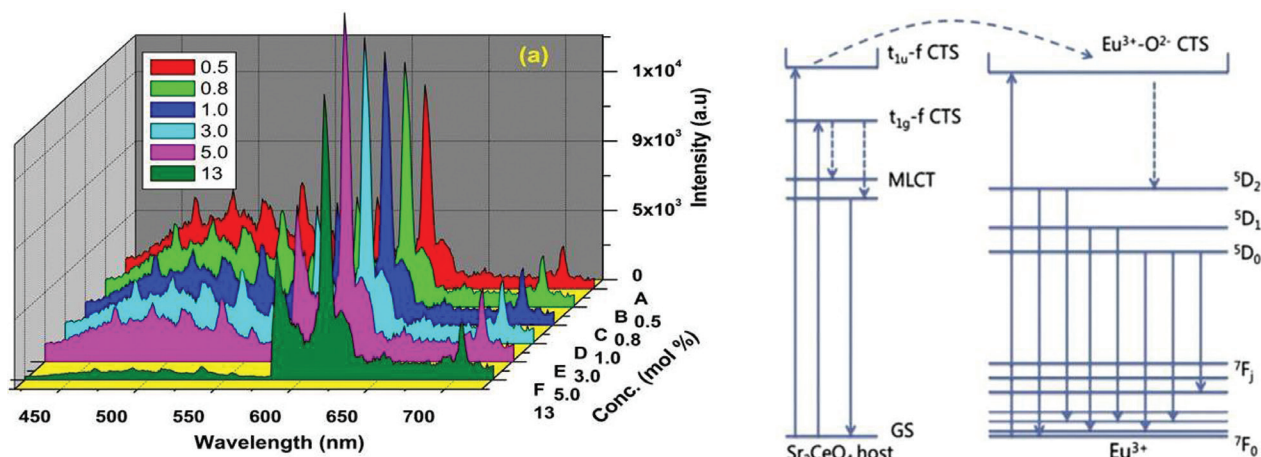
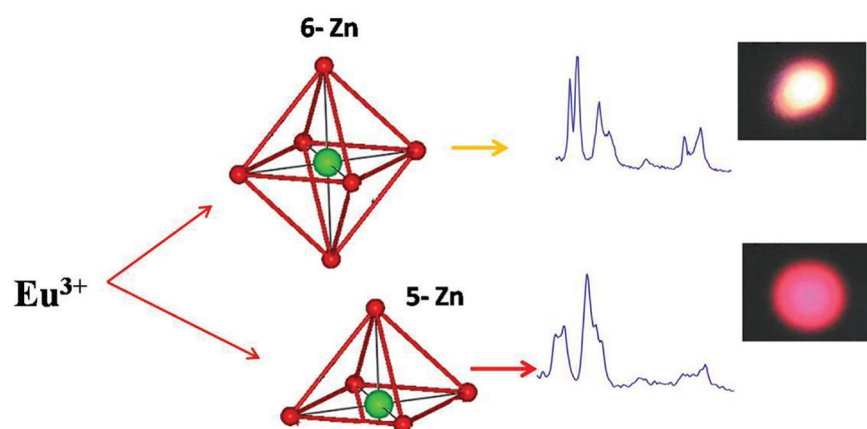


Fig. 5: Concentration dependence emission spectra and energy transfer mechanism



**Fig. 6: Structure dependent emission of europium ion in zincpyrophosphate**

higher than that of the species present in asymmetric environment which is consistent with the selection rules governing the transition.

Cost of lanthanide ion is an issue; keeping this in mind, we have synthesized rare earth free visible emitting luminescent materials viz.  $\text{SrZrO}_3$ ,  $\text{Sr}_2\text{CeO}_4$  and  $\text{Zn}_2\text{P}_2\text{O}_7$ . Hence, it is expected that suitable modification in the synthesis procedure as well doping these hosts with lanthanide ions can give efficient luminescent materials, which can have multi colour emission.

Effect of various synthesis conditions like concentration of dopant ion and annealing temperature on photoluminescence properties (emission spectra, excitation spectra and luminescence life time) of lanthanide were investigated. Based on critical distance calculations we have proposed mechanism for concentration quenching.

Based on concentration quenching, mechanism for the same is also proposed.  $\text{SrZrO}_3$  is an interesting host because of its multicolor emission properties and ferromagnetic behavior. EPR study showed the presence of oxygen vacancy in  $\text{SrZrO}_3$  nanocrystals. Emission and EPR studies along with theoretical calculations were carried out to bring out the possible reason for multicolor emission in  $\text{SrZrO}_3$

nanocrystals. Fig. 7 are plots of the temperature dependence of the resonance field position and line width of the ferromagnetic resonance (FMR) signal. The broad signal having a peak-to-peak linewidth of 3400 G was attributed to ferromagnetic resonance (FMR), which arises from transition within the ground state of the ferromagnetic domain. With the lowering of T, a broadening of the signal and a shift of the center of resonance to lower H values were observed. It may be mentioned that such a T-dependent change in the linewidth and line position of the resonance

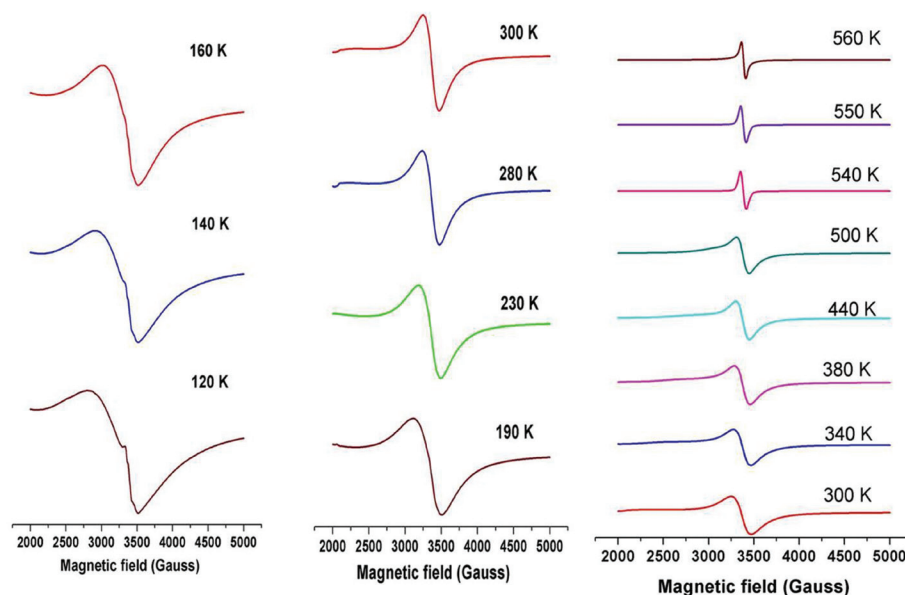


**Fig. 7: Temperature dependence of the EPR spectra of  $\text{SrZrO}_3$  in the range 160–560 K.**

signal would not occur in the paramagnetic state. The observed broadening of the signal and a shift of the center of resonance to the lower H values is attributed to the presence of a nonhomogeneous local magnetic field, which modifies both the resonance H and the line shape of the signal in the ferromagnetic state [18]. Low-field EPR spectra of the as prepared SrZrO<sub>3</sub> possess a large broad peak, conclusively showing that the spins in the system are strongly coupled and form spin clusters. The presence of the FMR signal even at 560 K indicated that the ferromagnetic TC for this sample is much above 500 K. These data clearly show that ferromagnetism persists well above room temperature. The strong temperature dependent effects occur in the ferromagnetic state because the field position and the line width depend on the magnetization and anisotropy constant, which are temperature dependent in a ferromagnet [19].

## References

1. Santosh K. Gupta, P. Ghosh, N. Pathak, A. Arya, V. Natarajan, *RSC Advances*, 4 ( 2014) 29202
2. Santosh K. Gupta, M.K. Bhide S.V. Godbole, V. Natarajan, *Journal of American Ceramic Society*, DOI: 10.1111/jace.13143, 2014
3. Santosh K. Gupta, R. Gupta, V. Natarajan and S.V. Godbole, *Materials Research Bulletin*, 49 (2014) 297-301
4. Santosh K. Gupta, R. Phatak, S.K. Thulasidas, V. Natarajan, *Advanced Science Engineering and medicine*, 6 (2014) 1-9
5. Santosh K. Gupta, M. Mohapatra, S. Kaity, V. Natarajan and S.V. Godbole, *Journal of Luminescence*, 132 (2012) 1329-1338
6. Santosh K. Gupta, M. Kumar, V. Natarajan and S.V. Godbole, *Optical Material*, 35 (2013) 2320-2328
7. Santosh K. Gupta, M.K. Bhide, R.M. Kadam, V. Natarajan and S.V. Godbole, *Journal of experimental Nanoscience*, 2013, DOI:10.1080 /17458080.2013.858833,
8. Santosh K. Gupta, N. Pathak, R. Gupta, S.K. Thulasidas, V. Natarajan, *Journal of Luminescence*, DOI: 10.1016/j.jlumin.2014.10.009
9. Santosh K. Gupta, M. Mohapatra, V. Natarajan and S.V. Godbole, *Journal of Materials Science*, 47 (2012) 3504-3515
10. Santosh K. Gupta, M. Mohapatra, V. Natarajan and S.V. Godbole, *International Journal of Applied Ceramic Technology*, 10 (2013) 593-602
11. Santosh K. Gupta, P. Ghosh, N. Pathak, A. Arya, V. Natarajan, *RSC Advances*, 4 ( 2014) 29202
12. Santosh K. Gupta, R.M. Kadam, V. Natarajan and S.V. Godbole, *Materials Science & Engineering B*, 183 (2014) 6-11
13. Santosh K. Gupta, M. Sahu, K. Krishnan, M. Saxena, V. Natarajan and S.V. Godbole, *Journal of Materials Chemistry C*, 1(2013)7054-7063
14. Santosh K. Gupta, N. Pathak, M. Sahu, V. Natarajan, *Advanced powder Technology*, 25 (2014) 1388-1393
15. Santosh K. Gupta, R.M. Kadam, P. Samui, V. Natarajan, S.V. Godbole, *Journal of Materials Research*, 28 (2013) 3157-3163
16. Santosh K. Gupta, R.M. Kadam, R. Gupta, M. Sahu, V. Natarajan, *Materials Chemistry and Physics*, 145 (2014) 162-167
17. Santosh K. Gupta, M. Mohapatra, V. Natarajan and S.V. Godbole, *RSC Advances*, 3 (2013) 20046-20053
18. M.K. Bhide, R.M. Kadam, A.K. Tyagi, K.P. Muthe, H.G. Salunke, S.K. Gupta, A. Vinu, A. Asthana, S.V. Godbole, *J. Mater. Res.*, 23 (2008) 463
19. F.J. Owens, *J. Phys. Chem. Solids*, 66 (2005) 793

# Design and Development of High Temperature $^{10}\text{B}$ Coated Proportional Counters for PFBR

**P.M. Dighe, D. Das, D.N. Prasad and L.P. Kamble**  
Electronics Division

*and*

**C.P. Nagaraj**  
Reactor Design Group, IGCAR, Kalpakkam

*and*

**R.K. Kaushik**  
Control Instrumentation Division

*and*

**S. Sarkar and S.S. Taliyan**  
Reactor Control Division

*and*

**P.P. Selvam, K. Binoy and N. Vijayan Varier**  
Technical Co-ordination & Quality Control Division

## Abstract

High sensitivity High Temperature Boron-10 Coated proportional Counters (HTBCCs) which can work in 250°C environment are developed for Fast Breeder Reactor. HTBCCs with sensitivity of 12 cps/nv, are used in Control Plug during initial core loading and first approach to criticality experiments to enhance the core monitoring, as Instrumented Central Sub-Assembly (ICSA) is lifted up and moved along with control plug away from the core region, during fuel loading. In case of an unforeseen long shutdown for more than 4 months, Shut Down Count Rate (SDCR) may become  $< 3$  cps. For the subsequent flux monitoring during fuel loading and start-up, it is required to use three boron coated counters (BCCs) with a sensitivity of 4 cps/nv. The detectors will be placed side by side at the spare detector location in Control Plug. HTBCCs of neutron sensitivity 12 cps/nv and one assembly containing three numbers of 4cps/nv detectors are developed and characterized for reactor applications. The functional tests and qualification tests were carried out on these detectors and the design specifications were established.

## Introduction

Neutron detectors capable of operating in high temperature environment are required in fast breeder reactors for reactor control and safety as part of nuclear instrumentation. The high temperature neutron detectors are used at above-the-core locations in the sodium pool for measurement of neutron flux from the fuel loading stage to the reactor power operation. The flux monitoring during fuel loading and approach to first criticality in fast breeder reactors is carried out using neutron detectors with sensitivity more than 10 cps/nv operating at

250°C continuously.  $^{10}\text{B}$  coated proportional counters are best suited for this requirement since compared to other detectors like  $^3\text{He}$  and  $^{10}\text{BF}_3$  proportional counters,  $^{10}\text{B}$  coated proportional counters have better tolerance to ambient gamma radiation, operate at lower bias voltages, and are non-corrosive in reactor environment. Earlier, high sensitivity ( $\sim 30$  cps/nv)  $^{10}\text{B}$  coated proportional counters has been developed but their maximum operating temperature is limited to about 120°C. The challenges of detector operation at high temperatures are overcome by advanced mechanical design and proper selection of construction material for long term continuous operation.  $^{10}\text{B}$

coated proportional counters with a sensitivity of 12 cps/nv are required for use at Control Plug locations of Prototype Fast Breeder Reactor (PFBR) for monitoring the flux during fuel loading / handling, approach to first criticality. In case of an unforeseen long shutdown for more than 4 months after source activation, the subsequent flux monitoring during reactor start-up is proposed to be carried out using boron coated counters with a sensitivity of 4 cps/nv operating at 250°C. The present article describes design, development and characterization of <sup>10</sup>B coated proportional counters of 12 cps/nv and 4 cps/nv thermal neutron sensitivity capable of operating upto 250°C developed for PFBR.

**Design**

Conventional boron coated proportional counters developed for reactor applications are of cylindrical shape as shown in Fig. 1. The outer cylinder acts as cathode. 94% enriched <sup>10</sup>B powder is mixed with binder and thinner and homogenous solution is prepared. Thin layer of this solution is coated on the inner surface of cathode and dried at 250°C. The process is repeated till desired coating thickness on the cathode surface is obtained. A very small diameter (thin) anode wire is mounted axially over insulators in the geometric centre of the detector. Heat shrinkable polyethylene sleeve is provided over the detector to isolate detector ground from the local ground.

For development of high temperature boron coated proportional counters, the following special design features have been incorporated.

- In conventional boron counters, polyethylene sleeve is provided over cathode tube for ground isolation. In the present detectors, cathode is encased in SS cylindrical housing insulated using alumina ceramic spacers for high temperature operation.
- Spring assembly made of spring steel is provided at one end of the detector assembly to absorb dimensional changes during temperature variation.
- Alumina ceramic spacers and feed throughs have been introduced as insulators instead of Teflon, Mylar insulators.
- The detector is constructed out of SS 304 L to minimize corrosion at weld joints.
- The detector is joined with triaxial mineral insulated cable for taking out the signal.

Incorporating above design modifications, two types of High Temperature Boron Coated proportional Counters (HTBCCs) have been developed. A 12 cps/nv HTBCC with 100 mR/h gamma tolerance is developed for measuring neutron flux during fuel loading operations. After long operation and long shut down of more than 4 months, for subsequent startup, high sensitivity boron counters for redundant safety channels are required with 4 cps/nv neutron sensitivity and 200 R/h gamma tolerance. For such requirements, three numbers of 4 cps/nv HTBCCs assembled in single housing have been developed. The fabrication of the detectors was carried at ECIL, Hyderabad. The main specifications of the detectors are given in Table 1. Fig. 2 and Fig. 3 give the construction schematic of the detectors.

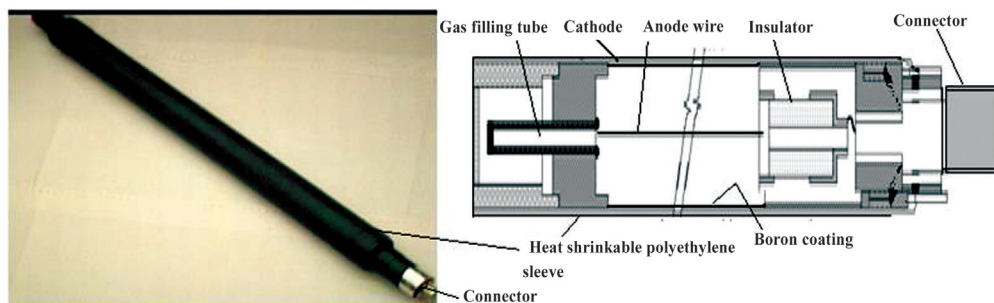


**Fig. 1: Picture and schematic of standard boron coated proportional counter**

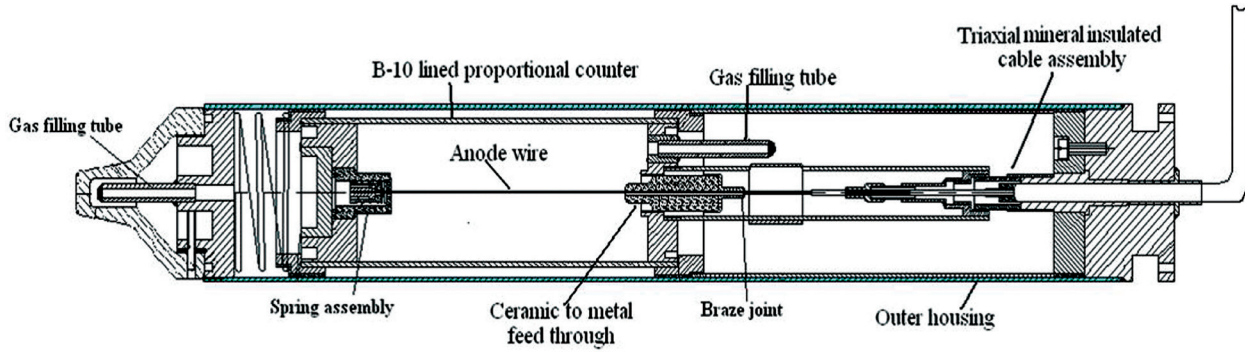


Fig. 2: Schematic diagram of High Temperature 12 cps/nv <sup>10</sup>B coated proportional counter

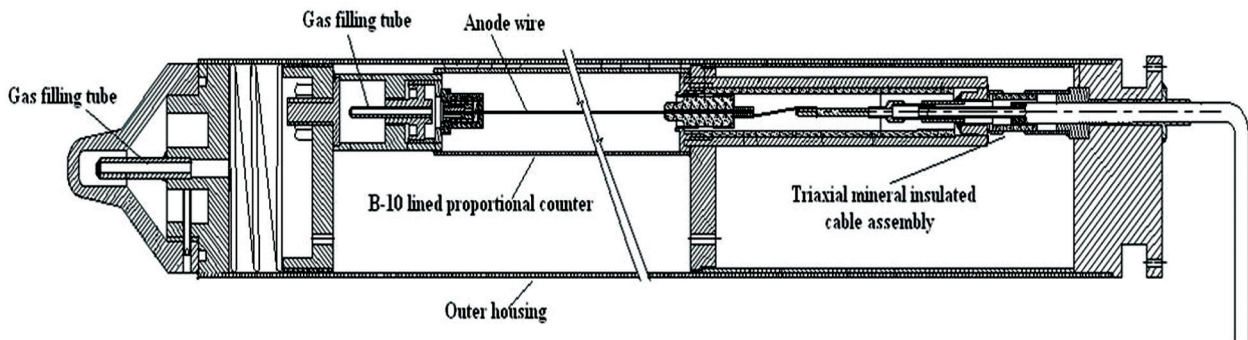


Fig. 3: Schematic diagram of High Temperature 4 cps/nv <sup>10</sup>B coated proportional counter (single detector)

Table 1: Main specifications of <sup>10</sup>B coated proportional counters

Detector	12 cps/nv	4 cps/nv
Outer housing material, overall dimensions	SS 304L; 1000 mm Long, 63 mm OD	SS 304L; 735 mm Long, 63 mm OD
Sensitive length	700 mm	378 mm
cathode	OD 54 mm, ID 51.3mm	OD 25.4 mm ID 23.8 mm (single detector)
Anode wire	25 μm dia. tungsten	
Filling gas	Ar (95%) + CO <sub>2</sub> (5%) at 18 cm Hg	
Cable and End connector	12 m long tri-axial Mineral Insulated cable having Triaxial bulkhead receptacle	
Neutron sensing material & coating thickness	94% <sup>10</sup> B enriched, 0.55 mg/cm <sup>2</sup>	94% <sup>10</sup> B enriched, 0.88 mg/cm <sup>2</sup>
Charge collection time	400 ns	200 ns – 350 ns
Operating voltage	800 V- 900V DC	750 V- 850 V DC
Measurement range	0.3 nv – 5x10 <sup>3</sup> nv	1 nv – 5x10 <sup>4</sup> nv
Operating temperature	250 °C	
Influence of gamma	upto 0.1 R/h without count loss	upto 200 R/h without count loss

**Design of cathode dimensions**

The requirement of neutron sensitivity in boron coated proportional counters governs the cathode dimensions. Elemental <sup>10</sup>B is coated on the internal surface of the cathode. Initially neutron sensitivity increases with increase in coating thickness. However, above an optimum coating thickness, the neutron sensitivity decreases due to self shielding effect. Therefore in boron coated proportional counter, the neutron sensitivity is directly proportional to boron coated surface area. The neutron sensitivity of boron counters can be derived from the following equation:

$$Sn = N \sigma \phi C \tag{1}$$

where  $N$  = number of <sup>10</sup>B atoms which is given as;  $N = S A t / a$  where  $A$  is Avogadro number  $6.023 \times 10^{23}/\text{mol}$ ,  $S$  is boron coated surface area,  $t$  is coating thickness in mass per unit area and  $a$  is atomic weight of boron,  $\sigma$  = reaction cross section,  $\phi$  = neutron flux and  $C$  = counting efficiency which depends upon the coating thickness. The efficiency  $C$  can be estimated from the following equations <sup>1</sup>:

$$C_{\alpha} = \frac{1}{2} \cdot \mu \cdot \left(T - \frac{T^2}{2R_{\alpha}}\right) \tag{2}$$

$$C_{Li} = \frac{1}{2} \cdot \mu \cdot \left(T - \frac{T^2}{2R_{Li}}\right) \tag{3}$$

where  $C_{\alpha}$  is efficiency for alpha particles emitted,  $\mu$  is attenuation coefficient,  $T$  is coating thickness,  $R_{\alpha}$  is range of alpha particles in the boron coating,  $C_{Li}$  is efficiency for lithium particles emitted,  $R_{Li}$  is range of lithium particles. The total efficiency  $C$  is the sum of efficiencies of both the particles and is given as

$$C = (C_{\alpha} + C_{Li}) \tag{4}$$

For cylindrical counters, if some neutrons have not interacted on one side of the coating, they may interact on the opposite coating while going from

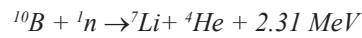
first coating surface to the second. Therefore, the efficiency in case of cylindrical counters is given by <sup>2</sup>

$$C_{cylindrical} = 2C - C^2 \tag{5}$$

Substituting numerical values, the neutron sensitivity of boron counters can be estimated and cathode dimensions are derived.

**Design of anode dimensions**

Neutrons interact with <sup>10</sup>B isotope ( $\sigma$  for thermal neutrons approximately 3836 barns) of boron coating and produce  $\alpha$  and lithium particles, which interact with gas and produce ionization.



The energy per neutron interaction produced is not sufficient to produce measurable pulse output. Therefore, it is required to amplify the primary charge produced by charge multiplication. This requires high electric field gradient. The high electric field in the cylindrical geometry detectors is produced by selecting very thin diameter anode wire. The charge multiplication coefficient,  $M$ , increases with increase in voltage applied to the anode. The total charge  $Q$  generated by  $n_0$  original ion pairs is  $Q = n_0 e M$  and the pulse amplitude  $V$  is given as

$$V = Q / C \tag{6}$$

where  $C$  is the capacitance of the detector.

Diethorn derived a widely used expression for  $M$  and is given as <sup>3</sup>

$$\ln(M) = \frac{V}{\ln\left(\frac{b}{a}\right)} \frac{\ln(2)}{\Delta V} \left( \ln\left(\frac{V}{pa \cdot \ln\left(\frac{b}{a}\right)}\right) - \ln(K) \right) \tag{7}$$

where  $p$  is gas pressure  $k$  is a Diethorn constant and  $\Delta V$  is ionization potential. The equation indicates that smaller is the anode wire diameter, greater

is the charge multiplication and hence the pulse output.

**Design of anode wire mounting assembly**

The anode wire chosen in proportional counters is always of a very small diameter to generate high electric field gradient for adequate charge multiplication. However, any small drift in anode wire position causes reduction in the gap between the cathode and anode. This happens especially at the ends of anode wire, where it is mechanically mounted over the insulator or at the centre, due to slackening. This position shift gives rise to generation of random breakdown pulses. Therefore, in order to avoid the breakdown to occur, it is very essential to have a very rugged anode wire mounting mechanism with appropriate insulator design for the proportional counters operating at elevated temperatures. For high temperature boron counters, a spring assembly using alumina ceramic spacers is designed<sup>4</sup>. The details of the spring mounting assembly are given in Fig. 4. The anode wire is kept at tension with the help of spring. The anode wire is enclosed with ceramic spacers and bushings and therefore even at elevated temperatures, the occurrence of breakdown phenomenon is avoided due to any differential dimensional variations.

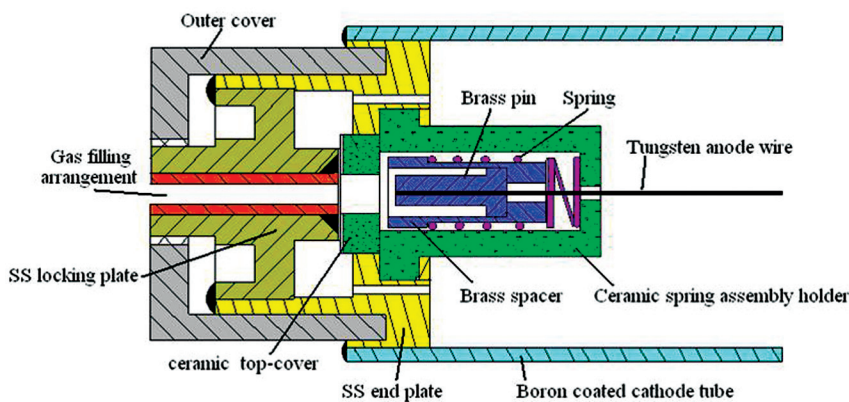


**Fig. 4: Anode wire mounting assembly**

**Detector design analysis for seismic event**

The mechanical integrity of the boron counters during specified seismic event is carried out by analysis using NISA finite element software version 11. The allowable initial tension in 25µm diameter anode wire was computed to be less than 20 gm at operating temperature of 250°C.

**Detector component cleaning procedure**

The cleaning of SS 304 L components is carried out using Trichloroethane, Perchloroethylene, Isopropyl Alcohol or Ethyl Alcohol and Acetone. After cleaning, the components are baked at 400°C. The ceramic components are cleaned in mild alkaline solution, heated upto 80°C and then rinsed in demineralized water. Cleaning is also done in ultrasonic cleaner in Acetone or aviation grade spirit without chlorides or fluorides. The ceramic components are then baked in oven up to 400°C for 2 hours duration just prior to taking up the assembly.

**Procedure for gas filling and gas filling tube pinching**

The welded detector is leak tested at 1.5 kg/cm<sup>2</sup> (abs) by pressure test and helium leak test up to 10<sup>-9</sup> std. cc /s. The detectors are evacuated and degassed by

baking at 250 °C till vacuum of the order of 10<sup>-6</sup> torr is achieved and maintained. After baking and degassing, it is ensured that the vacuum is maintained over a period of 12 hours before the gas mixture is filled in the detector. After gas filling, the filling tube is crimped with pinching tool and the pinched end is welded. The detector has all welded construction and all the weld

joints are Helium leak tested except for the pinched welded end of gas filling tube. Since the detector is filled at sub-atmospheric pressure, there is no known method to check the leak tightness of the crimped and welded end of gas filling tube. Therefore the leak tightness of the pinched end of gas filling tube has been ensured only by standardizing the crimping procedure. The gas filling tube made of SS 304L are annealed at 400°C for 90 minutes to normalize the stressed grains. The tubes are cooled in open furnace. Special pinching tool is designed which exerts a maximum torque of 10 kg-m. After pinching, the pinched end is inspected for uniformity of pinching as per standard procedure.

#### Tests and results:

Large sets of experiments were conducted on High Temperature Boron Coated Counter (HTBCC) to evolve data on the operation of detectors at 250°C.

#### Insulation Resistance and Capacitance

The bare 12 cps/nv HTBCC (without MI cable) showed 10 pF capacitance and  $\sim 10^{12}\Omega$  insulation resistance at 1kV DC at room temperature. No change in the insulation resistance and capacitance was observed at 250°C. The bare 4 cps/nv HTBCC (without MI cable) showed 8 pF capacitance and  $\sim 8 \times 10^{12}\Omega$  insulation resistance at 1kV DC at room temperature. No change in the insulation resistance and capacitance was observed at 250°C. 12 cps/nv and 4 cps/nv HTBCCs were then connected with 12 meter long integral triaxial mineral insulated cable. 12 cps/nv HTBCC with integral cable assembly showed 2.2 nF capacitance and  $\sim 10^{11}\Omega$  insulation resistance at 1kV DC at room temperature. At 250°C, the capacitance remained unchanged however the insulation resistance reduced to  $\sim 10^{10}\Omega$  at 1kV DC. 4 cps/nv HTBCC with integral cable assembly showed 2.2 nF capacitance and  $\sim 10^{12}\Omega$  insulation resistance at 900 V DC at room

temperature. At 250°C, the capacitance remained unchanged however the insulation resistance reduced to  $\sim 8 \times 10^{11}\Omega$  at 900 V DC.

#### Output pulse characteristics, neutron sensitivity and influence of gamma radiation at 250°C

The measured charge collection time for 12 cps/nv HTBCC ranges between 300 ns – 400 ns and for 4 cps/nv HTBCC ranges between 200 ns – 350 ns at room temperature. No measurable change in the charge collection time is observed while operating at 250°C. The neutron sensitivity of 12 cps/nv HTBCC and 4 cps/nv HTBCC was measured using a standard source of 27 nv thermal neutron flux. The average neutron sensitivity of 12 cps/nv HTBCC is 11.25 cps/nv ( $\pm 10\%$ ). The average neutron sensitivity of 4 cps/nv HTBCC is 3.7 cps/nv ( $\pm 10\%$ ). 12 cps/nv HTBCC was tested at 250°C with neutron source and in mixed radiation of neutron and 100 mR/h gamma radiation (Fig. 5 and Fig. 6). The variation in the count rate in plateau region is within 6 %. The voltage plateau data and discriminator bias data overlapped for room temperature and for 250°C. The variation in the count rate is within 10 % for 850 V and 900V HV. The observed discriminator bias plateau slope and voltage plateau slope was 1.3%/mV and 1%/ V respectively for 12 cps/nv HTBCC.

4 cps/nv HTBCC was tested at 250°C with neutron source and in mixed radiation of neutron and 200 R/h gamma radiation (Fig. 7 and Fig. 8). The variation in the count rate is within 5 % for 850 V HV and 80 mV discriminator bias. The voltage plateau data overlapped below 850 V at 250°C and 200 R/h gamma radiation. However after increasing the operating bias to 900 V, because of 200 R/h gamma radiation, increase in the count rate was observed. At room temperature, at 900 V HV the increase in count rate was 100% and at 250°C at 900 V HV the increase in count rate was 376% compared to the count rate without gamma radiation background.

This increase in count rate is attributed to the excess ionization produced by gamma radiation which increases magnitude of avalanches at higher operating voltages. Therefore it is recommended to operate the detectors at and below 850 V HV.

The discriminator bias curves plotted at 850 V show 5% variation in the count rate at 80 mV discriminator bias at room temperature and at 250°C in 200 R/h

gamma radiation. The gamma radiation produces additional ionization in the detector volume. This ionization creates space charge effects in the detector and due to this overall pulse amplitude reduces. However, in the plateau range the change in the count rate is within acceptable limit. The observed discriminator bias plateau slope and voltage plateau slope was 1.6%/10mV and 3.4%/10V respectively for 4 cps/nv HTBCC.

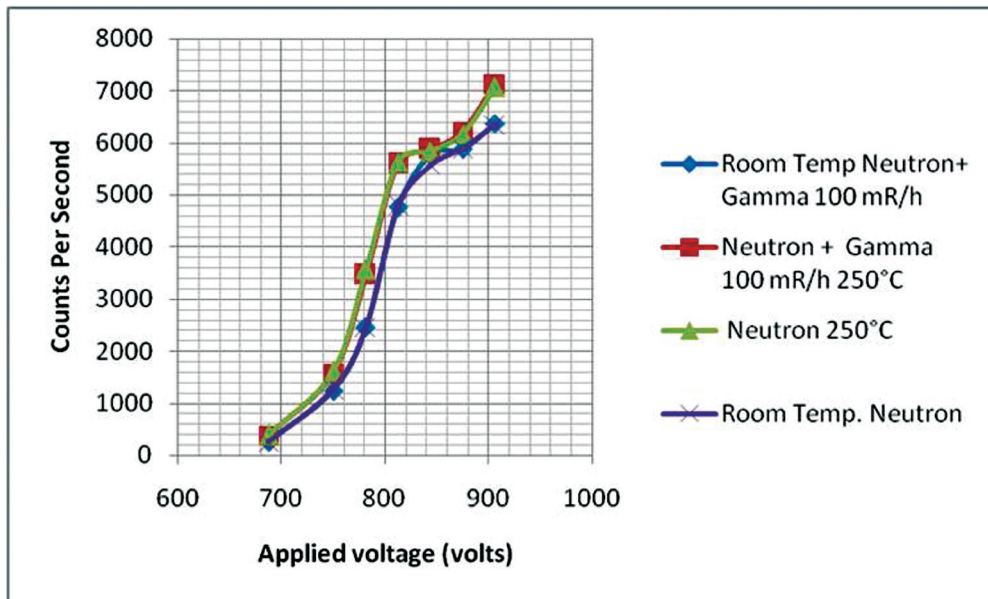


Fig. 5: Voltage plateau curve of 12 cps HTBCC in 100 mR/h gamma and 250°C

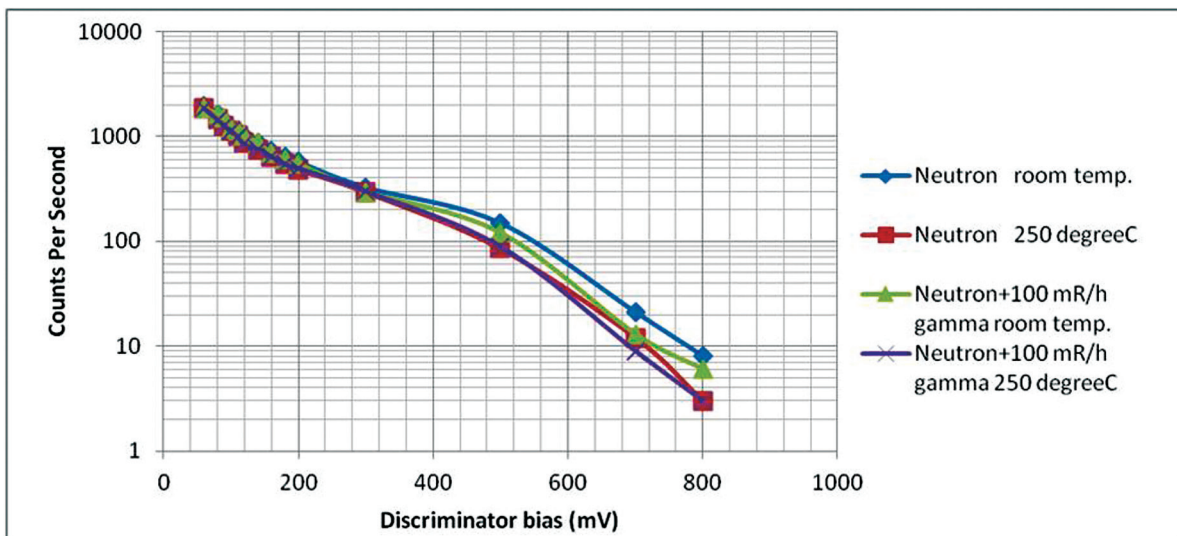


Fig. 6: Discriminator bias curve of 12 cps HTBCC in 100 mR/h gamma and 250°C

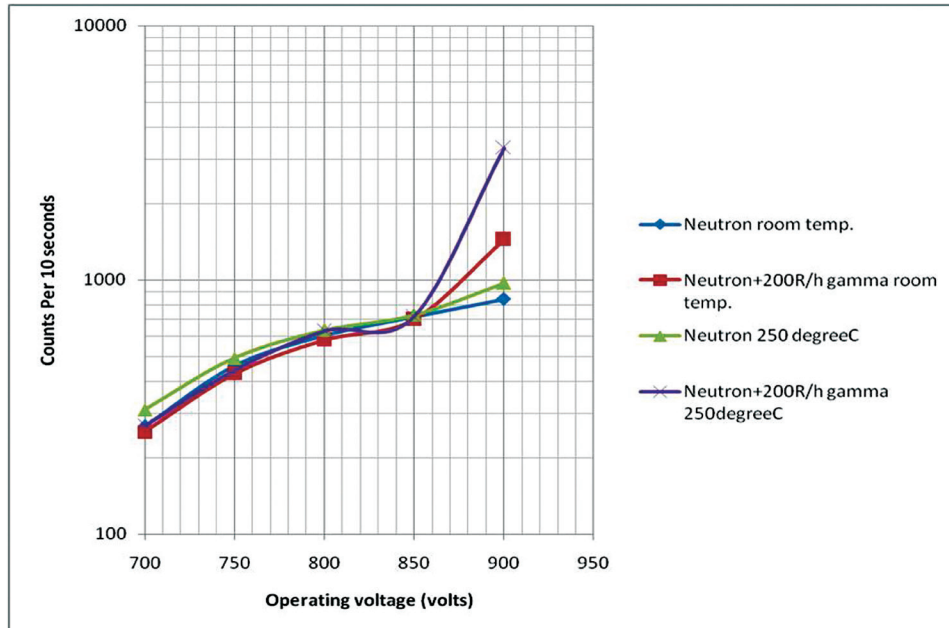


Fig. 7: Voltage plateau curves of 4 cps HTBCC in 200 R/h gamma and 250°C

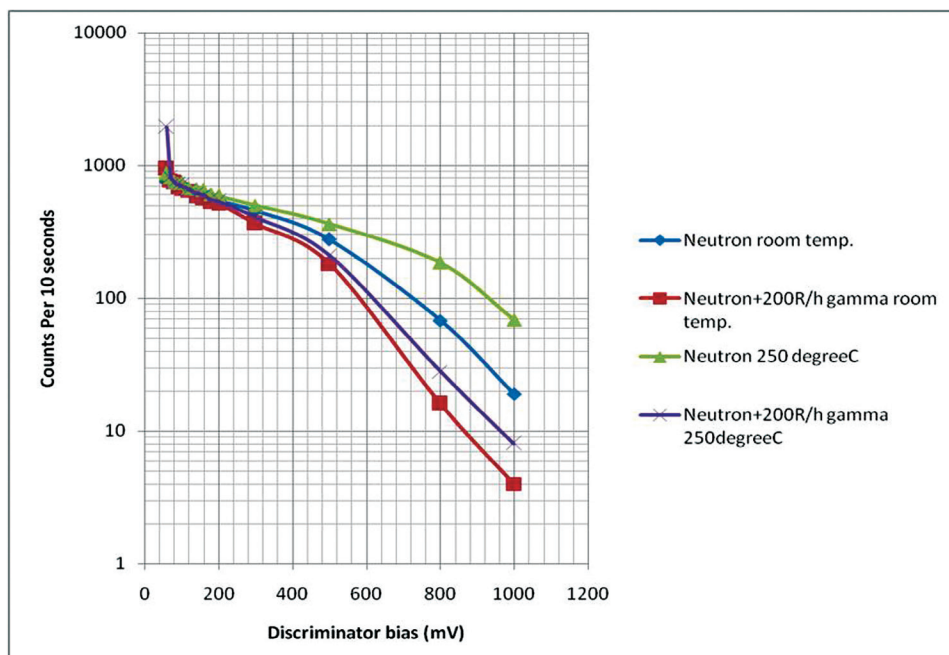


Fig. 8: Discriminator bias curve of 4 cps HTBCC in 200 R/h gamma and 250°C

**Count rate linearity w.r.t. neutron flux (in reactor)**

12 cps/nv and 4 cps/nv HTBCCs were tested for signal linearity (Fig. 9 and Fig.10) in AHWR-CF. 12 cps/nv

signal linearity is within 10% upto  $1.5 \times 10^3$  nv neutron flux and within 30% upto  $5 \times 10^3$  nv thermal neutron flux. 4 cps/nv HTBCC signal linearity is within 2% upto  $6 \times 10^4$  nv.

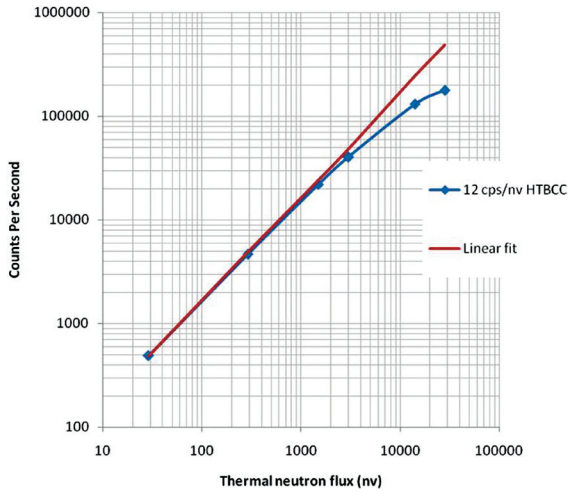


Fig. 9: Signal linearity of 12 cps/nv HTBCC in AHWR-CF reactor

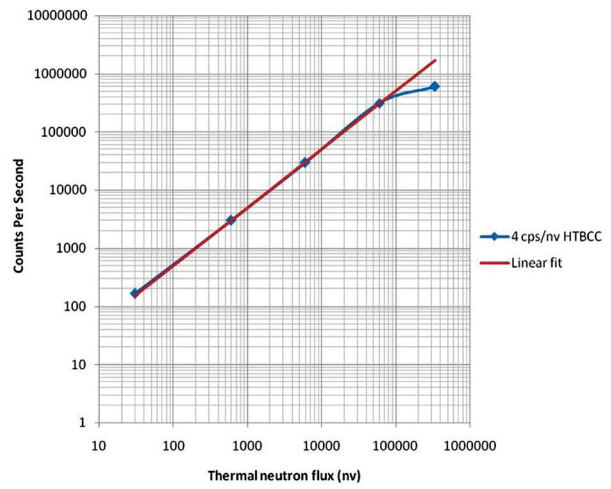


Fig. 10: Signal linearity of 4 cps/nv HTBCC in AHWR-CF reactor

**Qualification tests conducted on 12 cps/nv HTBCC**

Sample detectors from the production prototype lot of 12cps/nv HTBCC was subjected to various qualification tests viz. 12 number of thermal cycle tests at 250°C as shown in Fig. 11, vibration tests at 1-33 Hz and damp heat cycle tests as shown in

Fig. 12 (vide ref. PFBR/60510/SP/1008/Rev. 0). The detector was tested for functionality using 27 nv thermal neutron flux before and after the detector was subjected to qualification tests. Fig.13 and Fig. 14 give voltage plateau and integral bias curves of the detector and it was observed that the detector performance remained unchanged even after undergoing the above qualifications tests.

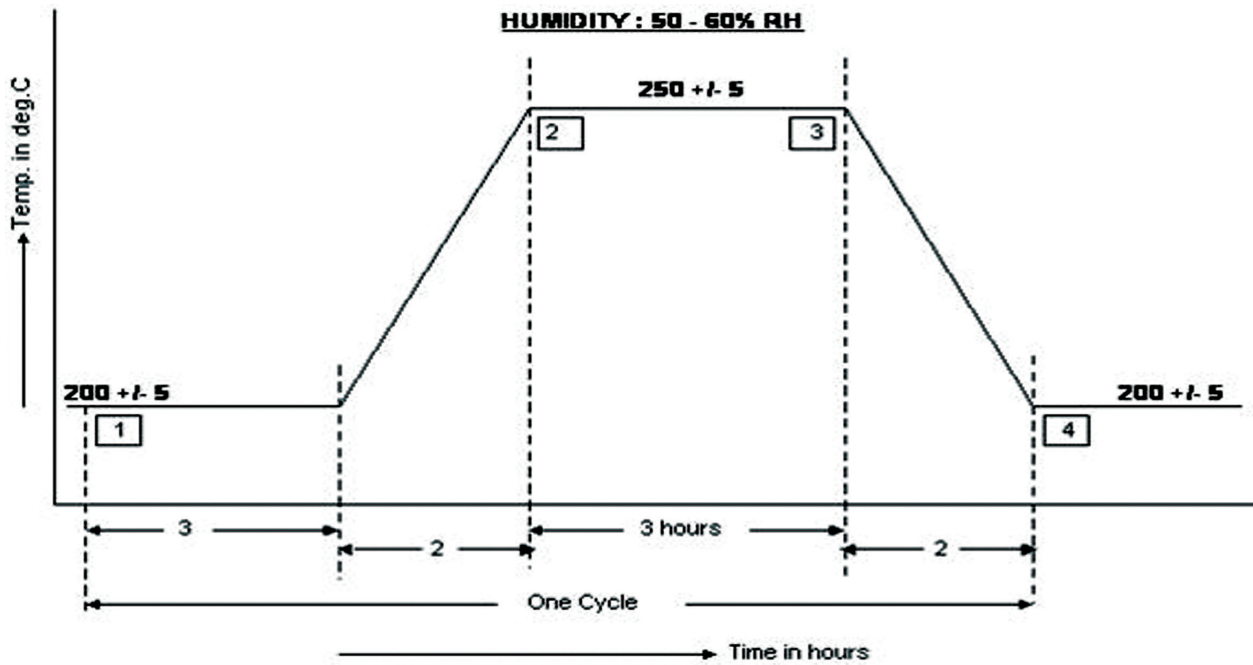


Fig. 11: Thermal cycle test profile

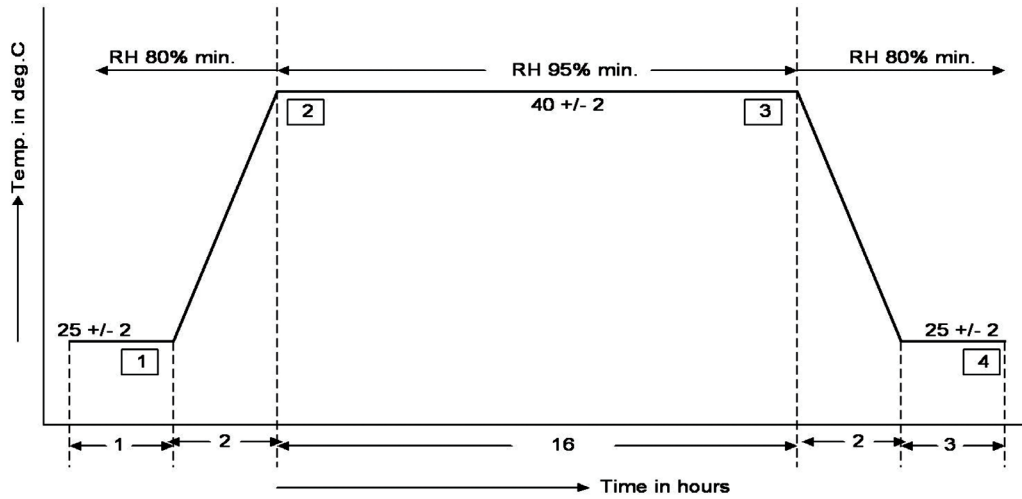


Fig. 12: Damp Heat Cycle Test profile

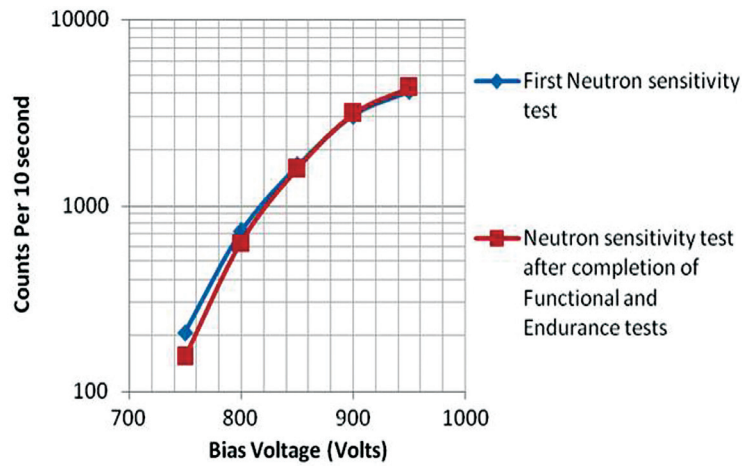


Fig. 13: Voltage plateau curves of 12 cps/nv HTBCC before and after subjecting to Functional & qualification tests

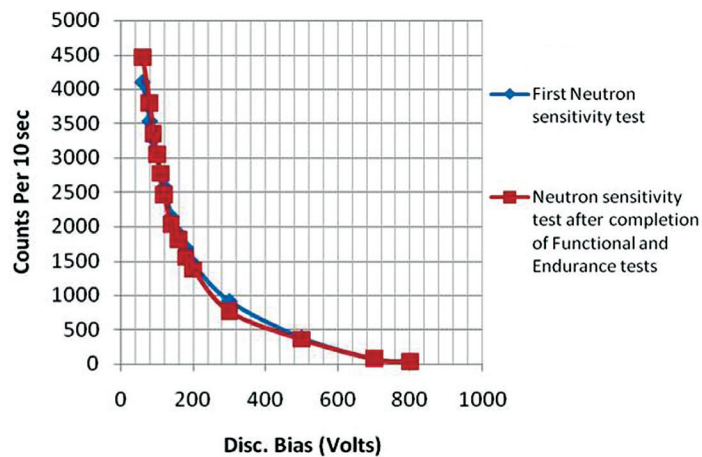


Fig. 14: Discriminator bias curves of 12 cps/nv HTBCC before and after subjecting to Functional & qualification tests

### Summary

12 cps/nv and 4 cps/nv High Temperature Boron Coated Counters (HTBCC) have been designed and fabricated. The fabrications of the detectors have been carried out at M/s ECIL, Hyderabad. The functional tests and qualification tests were carried out on these detectors to establish the design specifications. The performance tests conducted on the detectors showed that insulation resistance of the cable and detector upto 250 °C remains of the order of  $10^{10}$  ohms at 1 kV DC as required. The operating voltages of the detectors are observed to be as specified. The change in the neutron sensitivity up to 250 °C at the plateau range is negligible. The detectors' signal linearity is within  $\pm 10\%$  in the required range of operation. The detector performances remained unchanged after subjecting to qualification tests. After qualification of prototype detectors, 8 no. of 12 cps/nv and 6 no. of 4 cps/nv HTBCCs integrated with hangers have been fabricated and supplied to PFBR.

### Acknowledgements

The authors are thankful to Shri C.K. Pithawa, Director E&I and DM&A Groups and Dr. T.S.A. Krishnan,

Head, Electronics Division, BARC for encouragement and support in the work. Thanks are due to Shri A.K. Asthana, Head, RID, ECIL and his colleagues - Shri B. Krishnamurthy, Shri K.V. Rao, Shri Jayudu for fabrication and testing of the detectors. Thanks are also due to Shri V. Sathian and his colleagues from RP&AD for providing neutron and gamma source calibration facilities.

### References

1. R.D. Lowde, "The design of neutron counters using multiple detecting layers", *Review of Scientific Instruments*, 21 (1950) p.835
2. P.M. Dighe, D. Das, "Performance studies of boron lined proportional counters for reactor applications", *Nuclear Instruments and Methods in Physics Research A*, 770 pp. 29–35, 2015
3. G.F. Knoll, "Radiation Detection and Measurement", Third Edition, John Wiley & Sons; Inc., New York
4. P.M. Dighe, et. al., "Anode wire mounting technique for high temperature Boron-10 lined proportional counter", *Nuclear Instruments and Methods in Physics Research A*, 621 (1-3), pp. 713-715, 2010.

# Development of $\text{Gd}_3\text{Ga}_3\text{Al}_2\text{O}_{12}:\text{Ce}$ Single Crystal Scintillator and USB Based Portable Gamma-ray Spectrometer

M. Tyagi, S.G. Singh, A.K. Singh, D.G. Desai, B. Tiwari, S. Sen,  
R. Datta, S.C. Gadkari and S.K. Gupta  
Technical Physics Division

## Abstract

Crack-free single crystals of Ce doped  $\text{Gd}_3\text{Ga}_3\text{Al}_2\text{O}_{12}$  have been grown in Ar ambient using the Czochralski technique. These crystals were investigated with a view to improve the scintillation properties by a suitable post-growth annealing treatment. The  $\text{Gd}_3\text{Ga}_3\text{Al}_2\text{O}_{12}:\text{Ce}$  crystal scintillators having improved performances were coupled to a PMT to develop a portable gamma-ray spectrometer that could be powered from a USB port of a laptop. The scintillator crystal was also coupled to photodiodes and pulse height characteristics were measured for gamma-rays and charged particles in order to explore the possibility of fabricating detectors with a compact geometry.

**Keywords:** Crystal growth, Scintillator, Gamma - ray spectrometer.

## Introduction

The radiation detectors based on single crystal scintillators have several applications, including high-energy physics, medical imaging, geological exploration, nuclear industry and national security [1, 2]. Due to increasing applications, there is continuous demand and interest in the research for new scintillating materials with improved performances. In recent years, Ce doped materials have attracted the attention of many researchers due to their excellent combination of light output and decay time that involves allowed 5d-4f transition of these ions [3, 4]. Oxide crystals with a garnet structure have proven to be promising host materials due to their high density, broad transmission range and easy doping with rare earth elements like Ce [5, 6]. After Ce doped  $\text{Y}_3\text{Al}_5\text{O}_{12}$  (YAG) crystals were reported as scintillator detectors in electron microscopy by R. Atrata in 1978, significant material engineering by substituting different cations has been reported for

garnet compounds [7]. Recently, Kamada et al. have done extensive combinatorial band gap engineering for multi component garnet compounds [8]. The substitution of Gd or Ga sites with ions of different ionic radii in chemical formula of  $\text{A}_3(\text{B},\text{Al})_5\text{O}_{12}$  (where A: Gd, Y, or Lu and B: Ga, La, or Sc), alters the crystal field splitting of the Ce 5d states, and as a result the position of the lowest excited 5d states relative to the minima of the conduction band edge can be optimized for a better scintillation efficiency [8]. Therefore, optimization of different cation concentrations in the lattice could be made to alter the scintillation properties in a desirable manner. It was found that Ce doped  $\text{Gd}_3\text{Ga}_3\text{Al}_2\text{O}_{12}$  (GGAG) crystals have promising scintillation properties [9]. These crystals have a high density of  $6.7 \text{ g/cm}^3$ , high scintillation light output (LO) of over 45000 photons/MeV and a fast decay time of 55 ns [10].

In this communication, we describe a journey starting from the raw oxide materials to the development of a

USB based portable gamma-ray spectrometer based on single crystal scintillator of GGAG:Ce.

**Experimental**

Single crystals of Ce doped GGAG were grown using the Czochralski technique in an automatic diameter controlled crystal puller system (Model: Oxypuller, Cyberstar). The starting charge was prepared using solid state sintering of constituent oxides  $Gd_2O_3$ ,  $Al_2O_3$ ,  $Ga_2O_3$  in their stoichiometric molar ratio with 0.2 at% Ce doping. The sintering was carried in a box furnace at 1400°C. The formation of the single phase compound required for the melt growth was confirmed by X-ray powder diffraction measurements. As-prepared material in the form of pellets was loaded in a suitable crucible and heated to 50°C above its melting point to homogenize the melt. A single crystal seed (not oriented in a specific direction) was employed to initiate the crystal growth. A continuous flow of Ar through the closed growth chamber was maintained during the growth. The optimized parameters used for the growth of GGAG crystals are listed in Table 1.

**Table 1: Crystal growth parameters**

Melting temperature	1850°C
Pull rate	1 mm/h
Rotation rate	10-20 rpm
Initial chamber pressure	$1 \times 10^{-5}$ mbar
Ar gas pressure	1100 mbar
Temperature gradient	30-50°C/cm
Cooling rate	20-30°C/h

X-ray powder diffraction (XRD) measurements, to verify the phase of the starting material and the grown crystals, were carried out with Cu  $K\alpha$  radiation ( $\lambda=1.54056 \text{ \AA}$ ), employing Rigaku RINT 2000 diffractometer and scanning with a step size of 0.02° in the  $2\theta$  range from 10° to 90°.

Transmission/ absorption/ reflection spectra were measured with a Shimadzu 3600 UV-VIS-NIR spectrophotometer in the range from 185 nm to 800 nm. Photoluminescence (PL) properties were measured with an Edinburgh FLP-920 Spectro-fluorometer. The spectra were corrected for the spectral response of the source, monochromator and the PMT.

Light output and energy resolution measurements were made using a pulse processing chain consisting of a PMT, a pre-amplifier, a spectroscopic amplifier and an 8k MCA. The PMT was directly coupled to each sample using optical grease and a hemispherical Spectralon reflector to maximize the collection of light. The output of MCA was plotted in a graph where the abscissa represents the channel number corresponding to the light output from the crystal while ordinate shows the counts in a given channel. The scintillation decay was measured using a Tektronix digital oscilloscope.

**Results and Discussions**

**Optimization of composition and crystal growth**

X-ray diffraction pattern for Cerium doped gadolinium garnets  $Gd_3Al_xGa_{5-x}O_{12}$  (where  $0 \leq x \leq 5$ ) having different Ga/Al ratio are shown in Fig.1. The lattice

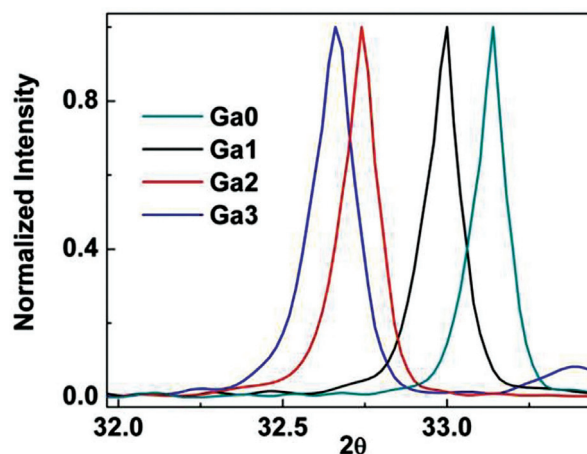


**Fig. 1: The effect of Ga concentration on X-ray diffraction peak of  $Gd_3Al_xGa_{5-x}O_{12}$  (where  $x = 2,3,4$  and 5).**

spacing variations as a result of partial or total Ga substitution at the Al site may be seen from a shift in the diffraction peak. The photoluminescence emission of Ce also shifts as a consequence of Ga substitution and therefore suggests a local re-adjustment of crystal field around the activator site.

The emission was found to shift towards higher energy (lower wavelength) by replacing Al cations with Ga as shown in Fig.2. This blue shift of Ce emission may be attributed to the replacement of smaller Al ions 0.54Å by bigger Ga ions 0.62Å. It may be understood with the help of the crystal structure of these compounds as shown in Fig.3. These materials crystallize in a cubic structure. The Gd/Ce is dodecahedrally coordinated with oxygen while Ga

and Al are coordinated with oxygen in octahedral and tetrahedral configurations. A bigger ion at Al sites causes the compression of adjacent dodecahedral around Gd/Ce ion and consequently changes the crystal field. A change in the crystal field splitting of Ce 5d levels changes the position of the lowest excited 5d level with respect to the conduction band leading to the blue shift in the emission. The position of the lowest Ce 5d level relative to the conduction band can therefore be optimized in such a way that helps to minimize the thermal ionization at room temperature by providing a sufficient gap but should not contribute to the negative effect of shallow traps due to the increased gap. Consequently, an enhancement in the scintillation light output could be obtained by altering the material composition. The optimized ratio of Ga/Al was found to be 3/2 for the best combination of light output and decay time. Therefore we have grown single crystals of ce doped  $Gd_3Ga_3Al_2O_{12}$  (GGAG) composition to fabricate radiation detectors.

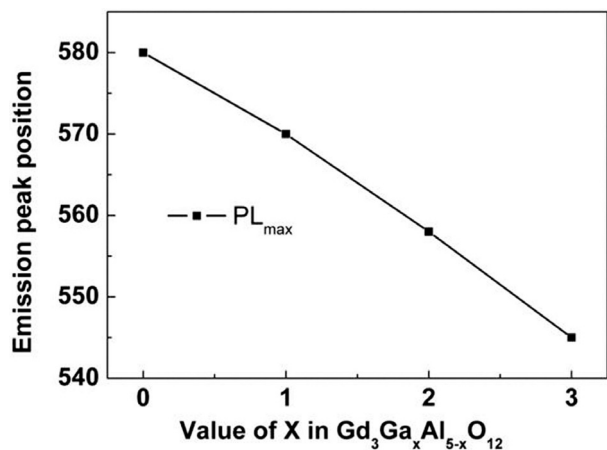


Fig 2: Effect of Ga concentration on the peak position of emission.

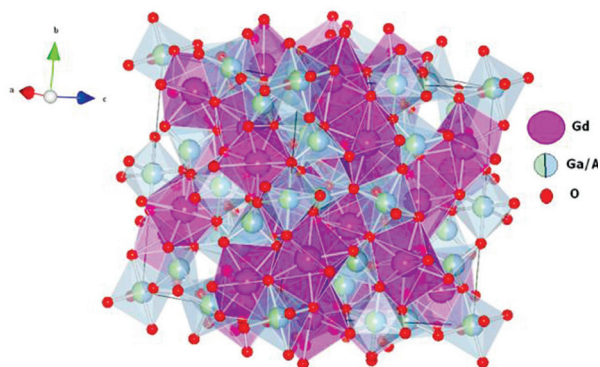


Fig 3: Crystal structure of  $Gd_3(Ga,Al)_5O_{12}$ .

Fig.4 shows photographs of an as-grown GGAG:Ce crystal having dimension of about 25 mm diameter and 60 mm length. The crystal gives a green fluorescence under the UV illumination due to an efficient emission from  $Ce^{3+}$  ions suggesting a

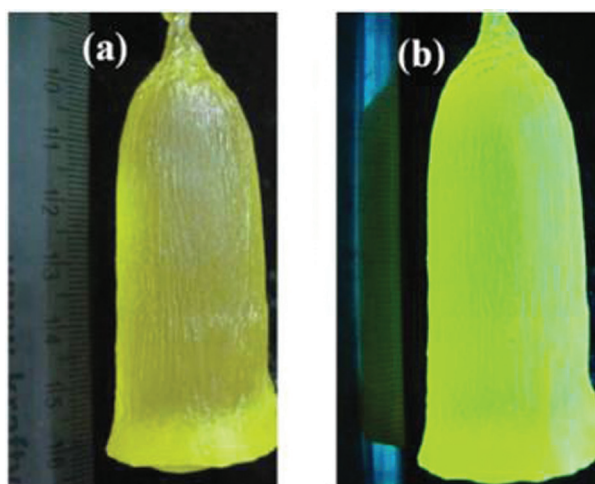


Fig 4: As-grown single crystal of GGAG:Ce in (a) day-light and (b) under UV illumination.

possibility of using photodiode as photo sensors with these crystals in order to fabricate compact detectors.

Fig.5 shows the transmission and emission spectra of GGAG:Ce crystal. The emission band due to the transition from the lowest excited 5d state to the ground 4f state of  $Ce^{3+}$  consists of two bands at 520 and 565 nm due to splitting of  $^4F_{5/2}$  and  $^4F_{7/2}$  ground state. The emission band lies in the transmission region of the crystal and therefore indicates less self absorption problem in these crystals. Therefore large size detectors can be fabricated using this material without self-absorption. The green emission from these crystals also matches well with the efficiency of photodiodes. This matching with photodiode enabled us to fabricate compact radiation detectors that operate at significantly lower voltages compared to a PMT.

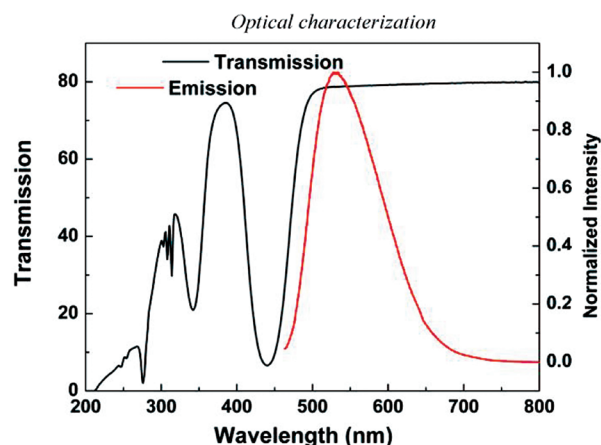


Fig 5: Transmission and emission spectra of GGAG:Ce crystal.

**Scintillation characterization**

The scintillation light yield measured from as-grown crystals was found to be much lower compared to the reported values. Since the crystals were grown in the Ar ambient, they are prone to have some oxygen vacancies and therefore post growth annealing treatments in air were performed to reduce the defect concentration.

Fig.6(a) shows the effect of annealing on the pulse height spectra of a  $^{137}Cs$  gamma source. The scintillation light output (LO) of the annealed crystals was found to increase after annealing the crystals in air at about  $1000^{\circ}C$  for 10 h. The results show that the oxygen vacancies could be effectively eliminated by the post growth annealing. The scintillation decay time was also found to improve after the annealing. The major component of the scintillation decay time was measured as 55 ns (Fig.6b). The improvement in scintillation properties after annealing the crystals in air confirms the role of defect centers related to the oxygen sub-lattice.

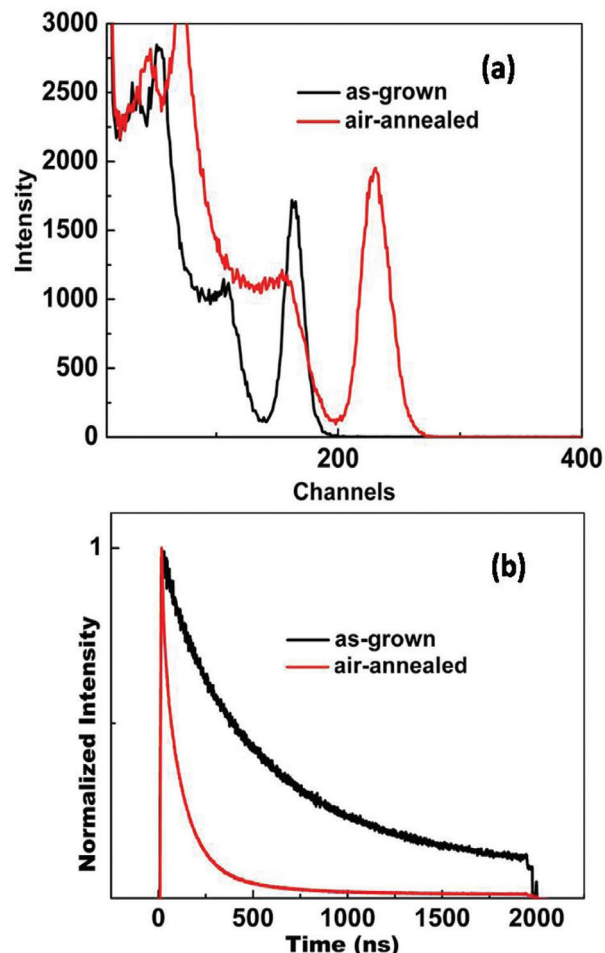
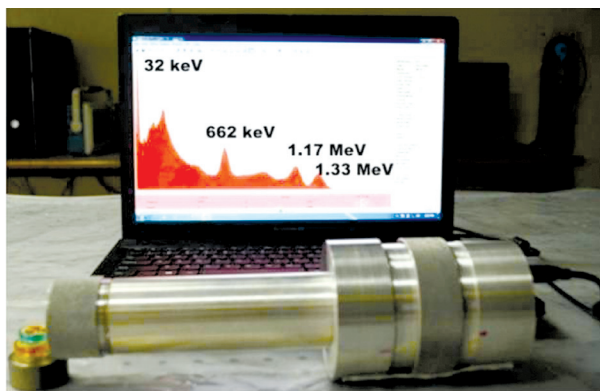


Fig 6: Effect of annealing on (a) relative light yield and (b) scintillation decay time of GGAG:Ce crystals.

### A USB powered detector Setup

A crystal sample with dimensions as  $18 \times 18 \times 10 \text{ mm}^3$  was cut from the annealed crystal. The sample did not have any visible inclusion or scattering centers. One surface was optically polished and coupled to a PMT having an active area of 1 inch diameter. The PMT output was given to a pulse processing assembly consisting of a pre-Amp, a shaping amp and an 8k MCA.

The power to all the components including HV to PMT was provided from a single USB port by employing necessary DC-DC converters. It made the whole set-up portable and convenient to use with a laptop as shown in Fig.7.



**Fig. 7: A USB based gamma-ray spectrometer developed using a GGAG crystal.**

The data processing was carried out by the Amptek DppMCA software. The setup was calibrated using  $\text{Cs}^{137}$  and  $\text{Co}^{60}$  sources and the performance was checked using sources of various other radio-active isotopes.

The parameters like shaping time of spectroscopic amplifier, PMT voltage and gain were optimized to get the well resolved pulse height spectrum. An energy resolution of about 4% has been achieved at 1332 keV gamma-ray from a  $\text{Co}^{60}$  source, as shown in Fig.8.

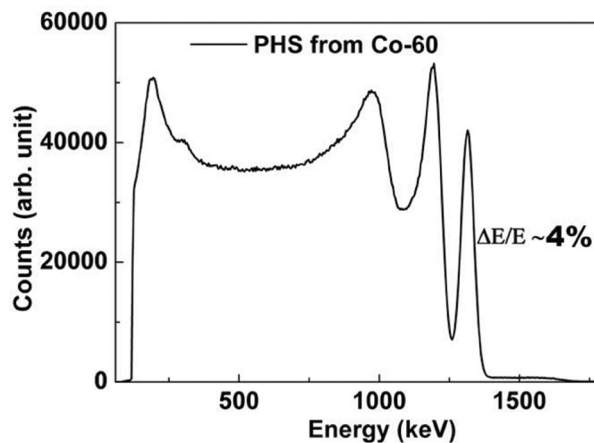


**Fig. 8: Pulse height spectrum of a Co60 source recorded using the GGAG crystal based gamma spectrometer.**

### Conclusions

Single crystals of Ce doped  $\text{Gd}_3\text{Ga}_3\text{Al}_2\text{O}_{12}$  crystals were successfully grown for gamma detection. The various characteristics of these crystals were investigated in details.  $\text{Gd}_3\text{Ga}_3\text{Al}_2\text{O}_{12}:\text{Ce}$  crystals grown in argon ambient have defects related to oxygen vacancies which could be eliminated by a post growth annealing treatment of the grown crystals. The light output and energy resolution were improved after annealing the crystal in air. After optimizing the scintillation parameter of the crystal, a portable detector has been fabricated which could be coupled to a USB based electronic set-up that does not need bulky high voltage power supplies or other NIM modules.

### References

1. Dujardin, C., et al., Optical and scintillation properties of large crystals. *Journal of Physics: Condensed Matter*, 1999. 10(13): p. 3061.
2. Melcher, C., Perspectives on the future development of new scintillators. *Nuclear Instruments and Methods in Physics Research Section A: Accelerators, Spectrometers, Detectors and Associated Equipment*, 2005. 537(1): p. 6-14.

3. Balcerzyk, M., et al., Future hosts for fast and high light output cerium-doped scintillator. *Journal of Luminescence*, 2000. 87: p. 963-966.
4. Baryshevsky, V., et al., Spectroscopy and scintillation properties of cerium doped YAlO<sub>3</sub> single crystals. *Journal of Physics: Condensed Matter*, 1999. 5(42): p. 7893.
5. Greskovich, C.D., et al., High speed, radiation tolerant, CT scintillator system employing garnet structure scintillators, 1991, Google Patents.
6. Drury, O.B., et al. Garnet scintillator-based devices for gamma-ray spectroscopy. in *Nuclear Science Symposium Conference Record (NSS/MIC)*, 2009 IEEE.
7. Autrata, R., P. Schauer, and J. Kuapil, A single crystal of YAG-new fast scintillator in SEM. *Journal of Physics E: Scientific Instruments*, 2001. 11(7): p. 707.
8. Kamada, K., et al., Composition Engineering in Cerium-Doped (Lu,Gd)(3)(Ga,Al)(5)O-12 Single-Crystal Scintillators. *Crystal Growth & Design*, 2011. 11(10): p. 4484-4490.
9. Mohit Tyagi, et al., "Effect of codoping on scintillation and optical properties of Ce doped Gd<sub>3</sub>Ga<sub>3</sub>Al<sub>2</sub>O<sub>12</sub> scintillators" *J. Phys. D: Appl. Phys.* 2013 46 475302 (12pp)
10. Samuel B. Donald, et al. "The Effect of B and Ca Co-Doping on Factors Which Affect the Energy Resolution of Gd<sub>3</sub>Ga<sub>3</sub>Al<sub>2</sub>O<sub>12</sub>:Ce", *IEEE Trans. Nuc. Science* 60 (2013) 4002-6.

## Third National Symposium on Advances in Control and Instrumentation (SACI- 2014): a Report

SACI-2014 was organized by the Reactor Control Division, BARC and was sponsored by the Board of Research in Nuclear Sciences (BRNS). It was held at the NPCIL auditorium, Nabhikiya Urja Bhavan, Anushaktinagar, Mumbai from November 24-26, 2014. The Symposium comprised ten sessions and 10 invited talks from subject experts. A total of 97 papers presented at the oral and poster sessions of the symposium, spanning a wide range of topics such as control theory, Control and Instrumentation (C&I) architecture applications and experiences, advances in tools and techniques, sensors, software security etc.

SACI 2014 was marked by active participation of a large number of delegates from various R&D institutions, industry and academia. SACI-2014 played a synergizing role in shaping the architecture of next generation C&I Systems in India. It also presented an opportunity to showcase Indian achievements and advances in the Control & Instrumentation sector and served as a platform to converge upon strategies in addressing future challenges in C&I sector such as rapid obsolescence of tools, techniques and components and ever-increasing demands in C&I software security.



Release of Book of Abstracts & Proceedings of SACI-2014: (L-R): Shri Y.S. Mayya, Head, RCnD & CnID and AD, E&I Grp., BARC, Shri C.K. Pithawa, Director, E&I & DMA Grps., BARC, Shri K.C. Purohit, C&MD, NPCIL, Dr. Sekhar Basu, Director, BARC, Shri A.G. Apte, Chairman, National Technology Research Organization, Dr. M.Y.S. Parsad, Director, Satish Dhawan Space Centre, ISRO and Dr. A.P. Tiwari, Outstanding Scientist, RCnD, BARC

## Theme Meeting on Application of Molecular Modeling in Separation Processes (AMMSP2015)

A one day theme meeting on “Applications of Molecular Modeling in Separation Processes” AMMSP2015 was organized at C Block Auditorium, BARC, Mumbai on January, 16, 2015. The meeting was organized by Chemical Engineering Division, BARC in association with Board of Research in Nuclear Sciences (BRNS), Department of Atomic Energy (DAE). The welcome address was given by Shri K.T. Shenoy, Head, ChED and Convener, AMMSP2015. In his speech Dr. S. L. Chaplot Director, Physics Group and Chief Guest for the meeting, stressed the needs of the multidisciplinary approach while solving practical problems. The meeting was inaugurated by Prof. Swapan K Ghosh, Raja Ramanna Fellow. Prof Ghosh gave an inaugural lecture on “Perspectives on theory and modeling of materials and processes”. He emphasized on the synergy between theory, computation and experiment in all branches of sciences and engineering for best conceptualization and successful implementation of a research programme and suggested a requirement of a suitable forum for hand shaking between

modelling and experiment. The proceedings of the meeting were released by Dr. Chaplot. The vote of thanks was delivered by Dr. Sk. Musharaf Ali, Head, LSS/ChED and Secretary, AMMSP2015. Presentations on various aspects of molecular modeling included application of the computational tool for selection of suitable ligand for the extraction of metal ion, An/Ln separation and isotope separation; design of low toxic drug molecules, nano particles and catalysts; fluid flow in nano tubes and metal organic framework for separation of fluids; thermodynamics of molten salt and Carbon nanotubes based adsorbents for An/Ln separation were presented. Experts from various institutes like ICT-Mumbai, IIT- Hyderabad, IIT-Mumbai and BARC made the presentation on these various aspects of the theme meeting. In the concluding session, a panel discussion was conducted where Prof. Dilip Maity, Associate Dean, HBNI stressed the needs of the platform where the modeling group and experimentalists can come together to solve the complex chemical separation processes of departmental needs.



Distinguished participants of AMMSP2015. Shri K.T. Shenoy, Head, ChED, Dr. S.L. Chaplot, Director, Physics Group, Prof. S.K. Ghosh and Dr. Sk. Musharaf Ali, Head, LSS/ChED at the inauguration of AMMSP2015.

## Conference on Nanomaterials and Technologies (CNT-2014): a Report

The 2<sup>nd</sup> International Conference on Nanotechnologies (CNT-2014) was held at the Vardhaman College of Engineering, Hyderabad on 17<sup>th</sup> and 18<sup>th</sup> Oct. 2014. The focus of the event, sponsored by BRNS, BARC, Mumbai, was on how nanotechnology could benefit humankind. The conference provided a platform to discuss current trends in nanotechnology that could translate into solutions for problems facing the environment, society and mankind at large. Scientists and Technologists and invited guest speakers discussed various nanotechnology solutions and environmental issues surrounding Nanotechnology at the conference.

There were seven technical sessions on Synthesis & Characterization of Nanomaterials, Nanocomposites and Sensors, Surface Films and Coatings and Nanoelectronics, including Oral Presentations and Poster Session. In his keynote address, Dr Henning ZoZ, ZoZ group, Germany spoke on Nanostructures in zero emission transportation, energy and economy. Dr Sunil Jai Kumar from the National Centre for Compositional Characterization of Materials, (NCCCM), BARC, Hyderabad, highlighted the challenges that researchers come across when characterizing Nanomaterials.



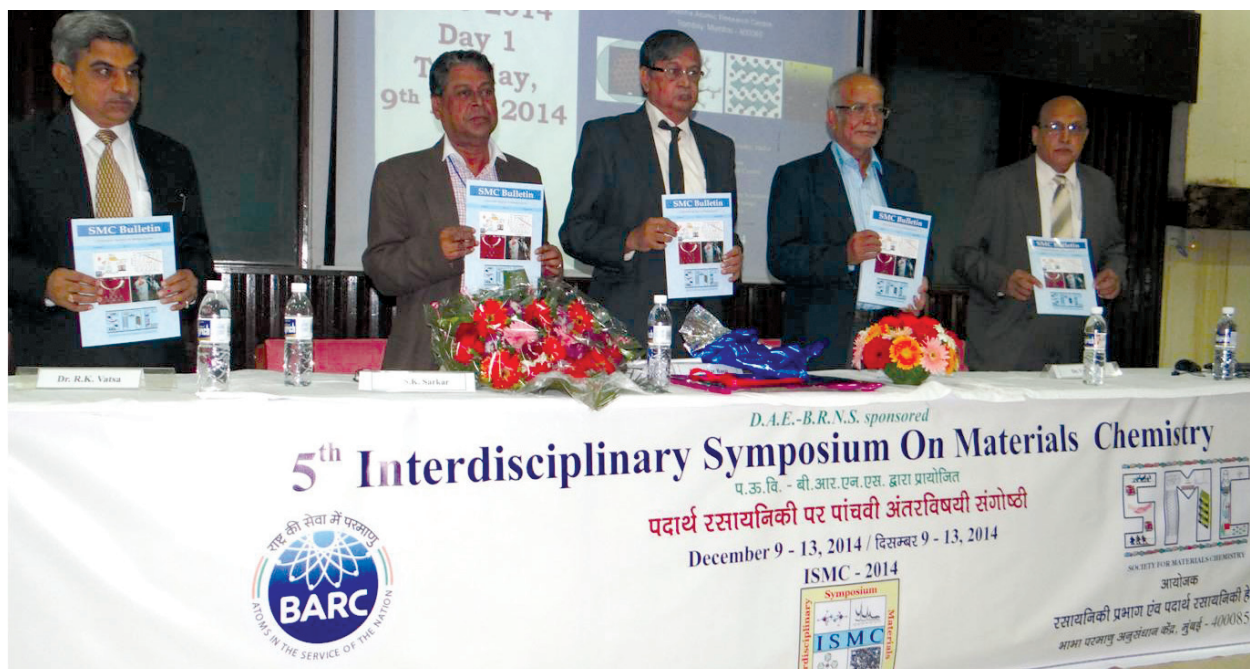
Inauguration of CNT 2014

## Report on DAE-BRNS 5<sup>th</sup> Interdisciplinary Symposium on Materials Chemistry (ISMC - 2014)

The DAE-BRNS 5th Interdisciplinary Symposium on Materials Chemistry (ISMC-2014), organized by the Chemistry Division and the Society for Materials Chemistry (SMC), was held at BARC during 9-13 December, 2014. The symposium was inaugurated by Dr. Sekhar Basu, Director, BARC. He also inaugurated the exhibition-cum-demonstration experiments section of the symposium. There was an overwhelming response from participants both from India and abroad. There were 38 invited talks and 360 contributed papers covering frontline research in diverse areas of materials science such as nuclear materials, nanomaterials, thin films, devices and sensors, materials for energy conversion and storage, biomaterials, magnetic materials, catalysts, soft matter, carbon-based materials, high purity materials, organic materials, computational materials chemistry and others. The deliberations were focused on materials research programme with a leaning towards materials

relevant to DAE programmes. The development of newer technologies based on nanomaterials for the above applications e.g. in separation science and sensors was discussed at large. Prof. H. W. Roesky, University of Goettingen, Germany, in his lead lecture highlighted the importance of materials chemistry in emerging technologies. In particular, he emphasized on low valent silicon which is a technical product for preparing silicon chips.

Speakers from India and abroad delivered invited talks on a wide variety of topics ranging from nanotechnology-driven cancer therapy, materials chemistry issues in fast reactors, energy conversion, nuclear fuels, solar cells, functional materials, complex chemical hydrides for hydrogen storage, diamond thin films for sensors, magnetic interactions in molecular systems, nanomaterials for ambient ionization, bridged fluorescent molecules as chemical sensors, Colloidal quantum dots,



From Left to Right: Dr. R.K. Vatsa, Secretary, ISMC, Dr. S.K. Sarkar, President, SMC, Dr. Sekhar Basu, Director, BARC, Dr. B.N. Jagatap, Director, Chemistry Group and Dr. V.K. Jain, Convenor, ISMC, at the inauguration function and the release of the SMC Bulletin

boron neutron capture therapy, cluster-based novel nanoscale materials, clinically useful metal oxides, semiconductor based flexible devices, for non-linear dielectric nano-crystals to high performance electrolytes for solid oxide electrochemical cells, advanced energy storage options for clean environment, nanomaterials for energy applications, thermochemical methods for hydrogen generation, and multi-components soft matter. In addition, there were 9 short presentations.

In a five-day long deliberations, 15 scientists from advanced countries like Germany, USA, Russia and South Africa, and 23 scientists from our national research centres, IITs, BARC, IGCAR, NIIST, IISc, Mumbai University and DIAT, delivered talks on their recent work. A total of 360 poster presentations, carried out on four consecutive days (9-12 December, 2014), were well attended by all the delegates with keen interest. Seven best posters were selected on each day for awards (90 posters per

day) by the expert committee. Valedictory session on 13th December, 2014 was presided over by Dr. B.N. Jagatap, Director, Chemistry Group. Prof. J.B. Joshi, Homi Bhabha Chair Professor, was the chief guest at the valedictory function. Many students, invited speakers and other delegates gave their feedback on the symposium. Information about the symposium was displayed by the Royal Society of Chemistry (RSC), UK on their website and it also sponsored two poster prizes for Best Posters. Further, RSC has consented to publish the papers presented by the invited speakers in the Journal of Materials Chemistry after peer review.

The deliberations and interactions among the delegates during ISMC-2014 may lead to several new BRNS projects as desired by various non-DAE delegates. A large participation of non-DAE delegates (about 275) in ISMC-2014 across different Indian states also indirectly served the purpose of outreach.

## Report on Nineteenth National Symposium on Environment (NSE-19)

The Nineteenth National Symposium on Environment (NSE-19) was held at the School of Environmental Sciences, Mahatma Gandhi University, Kottayam, Kerala during 11-13, December 2014. This symposium is jointly organized by School of Environmental Sciences, Mahatma Gandhi University, Kottayam and Health, Safety and Environment Group, Bhabha Atomic Research Centre, Mumbai and sponsored by BRNS / DAE. Prior to this, eighteen such symposia were held in various parts of the country. Considering the fact that climate change has been the major environmental issue and is currently the single greatest challenge facing environmental regulators the focal theme of the symposium was chosen as "Climate Change and its Impacts". Prof. C. T. Arvindkumar, Director,

School of Environmental Sciences, Mahatma Gandhi University welcomed the delegates of the symposium and highlighted the ongoing research activities of School of Environmental Sciences. Dr.(Ms.) G.G. Pandit, Head, EMAS, BARC and Convener, Symposium Organizing Committee talked about the theme of the symposium and outlined the National Symposium on Environment series being conducted earlier at different locations in India.

Dr. D. N. Sharma, Director Health Safety & Environment Group (HS&EG), BARC in his inaugural address, emphasized the importance of promoting nuclear energy as a clean and green energy option. He mentioned about the policies of the Department of Atomic Energy (DAE) which are in line with



Releasing of Proceeding of NSE-19 at the inaugural function (From left to right: Dr. E. V. Ramasamy, MGU; Dr. C.T. Arvindkumar, Director, SES, MGU; Dr. (Mrs.) G.G. Pandit, Head, EMAS, BARC; Dr. Babu Sebastian, Vice-Chancellor, MGU, Dr. D.N. Sharma, Director, HS&E Group, BARC; Dr. Kesav Mohan, Director, Institute of Climate Change, Kerala and Dr. Mahesh Mohan, MGU)



During the interactive section held on concluding day of NSE-19 (From left to right: Dr. C.T. Arvindkumar, Director, SES, MGU; Dr. (Mrs.) G.G. Pandit, Head, EMAS, BARC; Dr. D.N. Sharma, Director, HS&E Group, BARC; Dr. B.S. Tomar, Head, RACD, BARC and Dr. P.M. Ravi, Head, ESS, HPD, BARC)

deployment of clean technologies that involves carrying out environmental surveillance of all its projects during pre-operational, operational and post operational periods in order to ensure safety of the surrounding environment.

Dr. Babu Sebastian, Vice-Chancellor, Mahatma Gandhi University in his presidential address, highlighted the importance of environmental studies on climate change and forging alliances between academia and research institutes for national benefit.

There were more than 200 delegates across the country from various academic and research institutes apart from delegates from DAE units participated in the current symposium. The invited speakers for the symposium included experts from various research institutions including IITs and DAE units.

A wide range of topics related to environmental science and technology were covered during the

three-day symposium. It includes climate change and mitigation strategies, Environmental radioactivity including NORM, Speciation studies of toxic pollutants, Monitoring & modeling of pollutants and their transport, Environmental awareness, education and other related areas. There was lively interaction between young researchers and experts during poster sessions. Kudankulam Nuclear Power Plant (KKNPP) organised Public awareness programme during the symposium.

A one day workshop for capacity building in "Measurement of Kd (distribution coefficient) for toxic contaminants in geological matrices and its application in contaminant transport modeling" was also organized for the benefit of the delegates. An interactive session was also arranged to on the concluding day chaired by Dr. D. N. Sharma, Director Health Safety & Environment Group (HS&EG) for answering queries about the DAE activities with students from different universities.

## Technology Transfer to Industries

During the period between October 2014 and January 2015, BARC has transferred Six technologies to various industries. Technology Transfer & Collaboration Division (TT&CD) co-ordinated these technology transfers. The details are given below:

**A. "Stand-alone Solar Photovoltaic (PV) driven Battery-less Ultrafiltration (UF) Units for Water Purification." Technology was transferred to M/s M/s Aditi Solar Pvt. Ltd, Ranga Reddy Dist., (AP) on October 29th 2014.**

The technology of "Stand-alone Solar Photovoltaic (PV) driven Battery-less Ultrafiltration (UF) Units for Water Purification" has been developed by Desalination Division, BARC. These units are solar photovoltaic (PV) driven, battery-less, off-grid, stand-alone Ultrafiltration (UF) systems for water purification. On sunny days, they can be operated for 9 – 10 hours/day. They are capable

of removing un-dissolved species such as, dust, turbidity, microorganisms etc. from drinking water. These units are best suited for remote/rural areas where electricity is not available or the voltage is not stable. They can be used in urban areas also. As they are portable, they will be of great help for people working in desert areas, as in the case of defense personnel

**B. "Soil Organic Carbon Detection Kit (SOCDK)" technology was transferred to M/s Plasti Surge Industries Pvt. Ltd., Amravati (Maharashtra) on October 29th, 2014**

The technology of "Soil Organic Carbon Detection Kit (SOCDK)" has been developed by Nuclear Agriculture and Biotechnology Division, BARC. This kit analyses organic carbon content of soil directly on the field. This kit has been devised to help farmers to understand the carbon status of his field which

ultimately decides the yield of crop. It gives quick results and thereby enables farmer to take corrective measures for maintaining soil fertility especially before sowing and at the harvest of any crop. The detection method works on the basis of organic matter extraction from the soil. The extraction is enhanced by addition of chemicals provided in the kit. The colour developed after extraction shall be compared with chart provided for estimation of organic carbon content of the soil. Estimation of soil organic carbon content becomes easy to perform, giving immediate results and useful to farmers for their own use.



Photograph after signing the agreement with M/s Aditi Solar Pvt. Ltd, seen from left to right, Shri S.N. Dutta, TT&CD, Shri S. P. Mandala, Manager-SCM, M/s Aditi Solar Pvt. Ltd, Shri G. Ganesh, Head, TT&CD, Shri C. Sivaramaraju, Director, M/s Aditi Solar Pvt. Ltd, & Shri V. K. Upadhyay, TT&CD.

**C. “Dip N Drink Membrane Pouch” technology was transferred to M/s Plasti Surge Industries Pvt. Ltd., Amravati (Maharashtra) on October 29th, 2014**

The technology of “Dip N Drink Membrane Pouch” has been developed by Desalination Division, BARC. The Membrane Pouch is based on Osmosis process to get sterile drinkable solution from biologically contaminated water especially during disaster conditions like flood, cyclones, tsunami, earthquakes and useful for concentration of high value low volume product in food, pharmaceutical, chemical industries. It can also be used in Oral Rehydration Therapy in remote areas villages.



Photograph after signing the agreement with M/s Metalcrafts, Belgaum (Karnataka), seen from left to right, Shri V. K. Upadhyay, TT&CD, Shri S.N. Dutta, TT&CD, Shri Jagdeesh K. Chandran, CEO, M/s Metalcrafts, Shri G. Ganesh, Head, TT&CD, & Shri Chandan Gupta, DD.



Photograph after signing the agreement with M/s Plasti Surge Industries Pvt. Ltd., Amravati (Maharashtra) seen from left to right, Shri G. R. Ursal, TT&CD, Dr. R. C. Bindal, Head, MDS, DD, Dr. S. T. Mehetre, NA&BTD, Shri G. Ganesh, Head, TT&CD, Shri Kamlesh Daga, Director, M/s Plasti Surge Industries Pvt. Ltd., Ms. Saloni Daga, Marketing Executive, M/s Plasti Surge Industries Pvt. Ltd. & Shri V. K. Upadhyay, TT&CD.

**D. “Solar Energy Driven Portable Domestic Brackish Water Reverse Osmosis (BWRO)” technology was transferred to M/s Metalcrafts, Belgaum (Karnataka) on January 5th 2015**

The technology of “Solar Energy Driven Portable Domestic Brackish Water Reverse Osmosis (BWRO)”

has been developed by Desalination Division, BARC is based on solar photovoltaic (PV) system hence it is battery-less, off-grid/stand-alone. It has capacity of 10 litres/hr (lph) which can desalinate contaminated water of salinity 1000 - 3000 ppm (mg/lit) to provide drinking water of 50 - 300 ppm. The product water will be devoid of toxic elements, pathogens & turbidity too. It is best suited for remote/rural areas where electricity is not available or the voltage is not stable. It can be used in urban areas also. As it is portable, it will be of great help for the people working in desert areas especially in the case of defence personnel.

**E. “Distress Alarm Device - NIRBHAYA GSM” Technology was transferred to M/s. Triumph Design Corporation, Goregaon (E), Mumbai on January 12th, 2015.**

BARC has developed a GSM based Distress Alarm Device called “NIRBHAYA-GSM”. The user can send an SMS to his/her near and dear ones, when in distress using this instrument. The instrument



Photograph taken during the occasion of signing the agreement with M/s. Triumph Design Corporation, Goregaon (E), Mumbai seen 1st row from L-R, Shri G. R. Ursal, SO/F, TT&CD, Shri Hiren R. Panchal, Partner, M/s. Triumph Design Corporation, Shri Ramesh D. Panchal, R&D Head, M/s. Triumph Design Corporation, Shri Kamal R. Panchal, Partner, M/s. Triumph Design Corporation, Shri C.K. Pithawa, Director, E&I Group, Shri G. Ganesh, Head, TTCD, Shri D. Das, Head, ED, Shri Shailesh Khole, SO/G, ED

2nd row from L-R, Shri S.K. Lalwani, SO/G, Shri Sandeep Bharade, SO/F, Shri Vineet Sinha, SO/F, Shri Gopal Joshi, SO/H, Shri Rajesh Kumar Jain, SO/F, Smt. Shikha Shrivastava, SO/D all are from ED.

can be programmed to send SMS to up-to five user-defined numbers. The Distress SMS includes the users name, age, sex, blood group, and specific medical condition if any, in addition to the current GPS location of the user. User can also include conditions like "allergies to a particular medicine" in the medical condition while programming the instrument. The instrument can also respond to the queries from any one of the predefined numbers regarding the current user location. This is very useful in case of children or young persons who might be kidnapped or under distress but cannot use the instrument. It can be used for tracing goods & vehicles. This would also be beneficial for old persons suffering from memory loss conditions like Alzheimer or Parkinson.

**F. Nisargruna Biogas Technology based on biodegradable waste has been developed by NA&BTD. The plant processes biodegradable waste into biogas and weed free manure. It was transferred to the following five parties :-**

- Dr. B R Ambedkar Institute of Technology, Port Blair, A&N Islands on 28.10.2014
- M/s Sustainable Biosolutions LLP, Goa on 31.11.2014
- M/s NCM-Shoava Engineers Pvt. Ltd., Indore on 02.12.2014
- M/s Chokhi Dhani Resort Pvt. Ltd., Jaipur on 02.12.2014
- M/s S K Renewables Pvt. Ltd., Hyderabad on 12.01.2015

## Report of 5<sup>th</sup> Conference on Neutron Scattering (CNS2015)

The 5th Conference on Neutron Scattering was held at the Homi Bhabha Centre for Science Education (HBCSE), Mankhurd, Mumbai, during February 2 - 4, 2015. It was sponsored by the Board of Research in Nuclear Sciences, and organized by BARC in association with the Neutron Scattering Society of India (NSSI). Dr. S.L. Chaplot, Director, Physics Group, BARC inaugurated the conference, while Prof. V. C. Sahni, Former Director, Raja Ramanna Centre for Advanced Technology was the chief guest of the inaugural function. Dr. R. Mukhopadhyay, President, Neutron Scattering Society of India, and Head, Solid State Physics Division, delivered the presidential address, and Dr. R. Mittal, convener, CNS2015, conducted the inaugural function.

There were nearly 135 participants including 9 invited speakers from abroad (USA, France, UK, and Australia). During the three days conference, 35 invited talks were delivered, and 100 posters were presented. An evening talk on "A Story of Neutrons from Trombay" was delivered by Dr. B.A. Dasannacharya, Former Director, UGC-DAE CSR and Solid State & Spectroscopy Group, BARC. He brought out the glimpses of neutron scattering from the early days of the Atomic Energy Establishment Trombay (later renamed as BARC).

The conference covered all the major areas of neutron based multidisciplinary research including neutron

facilities, science and its applications. A particular emphasis was given on strongly correlated electron systems, critical phenomena and magnetic phase transitions, functional materials, nanomaterials, soft matter and biological systems, energy and green materials, thin films and multilayers, and neutron instruments. The conference provided very useful scientific discussions and platform for initiating collaborations among the national and international neutron scattering researchers. In order to encourage young scientists/students working in the area of neutron scattering, 5 best poster awards, sponsored by the NSSI, were given.

Researchers from various universities and national institutions utilize the National Facility for Neutron Beam Research (NFNBR) at Dhruva reactor, BARC regularly. To promote an enhanced utilization of the NFNBR, a pre-conference Neutron School was jointly organized by BARC and UGC-DAE CSR, Mumbai Centre during January 27 - 31, 2015 at BARC. The Neutron School included hands-on experiments at the Neutron scattering facility at Dhruva, besides giving a flavour of theory and data analysis. Apart from the faculty of BARC and UGC-DAE CSR, some of the foreign invited speakers to the conference also delivered lectures in the School. The School was extremely beneficial to the participating students and faculty members from various universities.



A group photograph of the participants of the CNS2015

## 59<sup>th</sup> DAE Solid State Physics Symposium-2014

The 59th DAE Solid State Physics Symposium-2014 was held at VIT University, Vellore, Tamil Nadu during December 16-20, 2014, and it was fully sponsored by the Board of Research in Nuclear Sciences. There was an overwhelming response from various individuals, institutions and research groups across the country for participation in this symposium. Total 1381 submissions were received which included 1333 contributed papers, 38 Ph. D theses, and the contributions from 10 young achiever award (YAA) nominees. Out of these, 854 submissions were accepted for presentations.

The topics covered in this symposium through 54 invited talks, 24 oral presentations, and over 800 poster presentations were: (a) Phase Transitions, (b) Soft Condensed Matter including biological systems, (c) Nano-materials, (d) Experimental Techniques & Devices, (e) Glasses & Amorphous Systems, (f) Surfaces, Interfaces & Thin Films, (g) Electronic Structure & Phonons, (h) Single Crystals, (i) Transport Properties, (j) Semiconductor Physics, (k) Superconductivity, Magnetism and Spintronics, and (l) Novel Materials. Besides there were thematic seminars on (i) Crystallography, (ii) Science with INDUS-1 & (iii) INDUS-2 Synchrotron Radiation Sources, (iv) Computational Condensed Matter Physics, (v) Thermoelectric Materials and Devices, (vi) Science with the National facility for Neutron beam Research, (vii) Multifunctional Materials/Multiferroics, (viii) Thin Film Multilayer Devices, (ix) Magnetism & Superconductivity, (x) Organic/Soft Matter, (xi)

Dielectric/Piezoelectric Materials and (xii) Nano Materials, Nano structures & Devices.

The symposium was inaugurated by Dr. S.L. Chaplot, Director, Physics Group, BARC. In the inaugural address, his emphasis on promoting a well-conceived basic research leading to an applied technology was highly appreciated by the scientific community and the media. The inauguration session was followed by two special plenary talks; (i) one on "Electrical and optoelectronic measurements on a single nanowire: Solid-state physics at a new scale" by Prof. A.K. Raychaudhuri, S.N. Bose National Centre for Basic Sciences, Kolkata, and (ii) the other on "Structure, magnetism and superconductivity in  $\text{BaFe}_2\text{-xRuxAs}_2$ " by Dr. C.S. Sundar, J.C. Bose Fellow, IGCAR, Kalpakkam.

Two special evening talks were delivered: (i) "Sciotoons and Nanotechnology: A small science for a big change" by Prof. P.K. Srivastava, CSIR-Central Drug Research Institute, Lucknow, and (ii) "Clean Energy Technologies : Challenges & Prospects" by Dr. V.C. Sahni, Ex-Homi Bhabha Chair Professor, DAE. The valedictory session was chaired by Dr. V.C. Sahni who in his concluding address summarized the five-day events.

In this symposium 26 awards were given which included 20 best poster presentation awards, 3 Young Achiever's Awards, 3 Best Thesis Awards. On this occasion, a special souvenir was brought out in collaboration with the Indian Physics Association (IPA). A special presentation stall was also arranged to highlight BARC's outreach programmes.



Inaugural address by Dr. S.L. Chaplot, Director, Physics Group, BARC



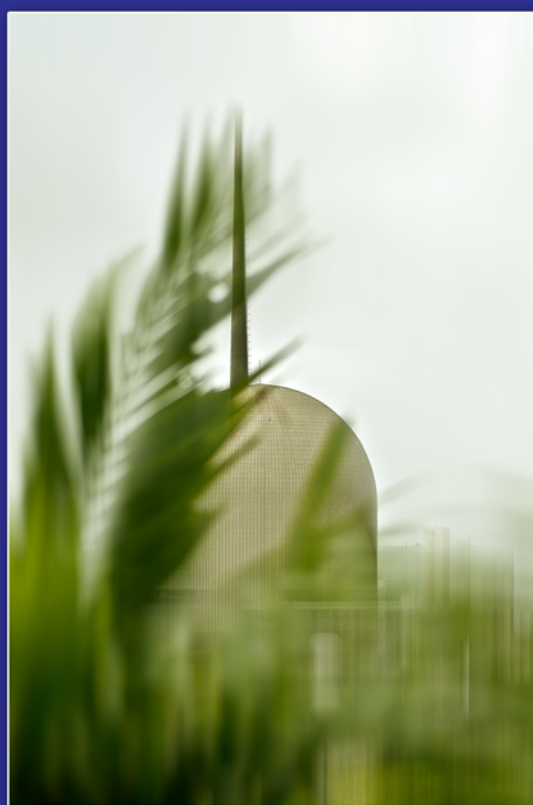
Welcome address by Dr. N.K. Sahoo, the Convener of the Symposium

## BARC Scientists Honoured

Name of the Scientist : P.K. Pujari  
Affiliation : Radiochemistry Division  
Name of the Honour : Elected Chairperson of the 12-member International Committee on Positron and Positronium Chemistry for a 3-year period from November 2014.

Name of the Scientists : S.M. Toprani and Birajalaxmi Das  
Affiliation : Radiation Biology & Health Sciences Division  
Name of the Award : Young Scientist Award  
Title of the Paper : Radio-adaptive Response of Base Excision Repair Genes & Proteins in resting Human Peripheral Blood Mononuclear Cells exposed to Gamma radiation  
Presented at : International Conference on Radiation Biology (ICRB), New Delhi, Nov. 11-13, 2014.

Name of the Scientists : Jyothi Sharma, T. Mahata, R.C. Hubli\*, P.K. Patro, Deep Prakash and P.K. Sinha  
Affiliation : Powder Metallurgy Division and Materials Processing Division\*  
Title of the Paper : "Influence of Lanthanum Site Deficiency on Phase Stability and Electrical Conductivity of  $(\text{La}_{0.75}\text{Sr}_{0.25})_{1-x}\text{Cr}_{0.5}\text{Mn}_{0.5}\text{O}_{3-\delta}$  in air and hydrogen atmosphere"  
Name of the Award : Best Paper Award (Second Prize)  
Presented at : DAE-BRNS 5<sup>th</sup> Interdisciplinary Symposium on Materials Chemistry (ISMC-2014) held at BARC, Mumbai durinn Dec. 9-13, 2014.



The CIRUS Research Reactor at BARC

Edited & Published by :

Dr. G. Ravikumar

Head, Scientific Information Resource Division

Bhabha Atomic Research Centre, Trombay, Mumbai 400 085.

BARC Newsletter is also available at URL: <http://www.barc.gov.in>